

THE LARGE SCALE STRUCTURE OF THE UNIVERSE

GUIDO CHINCARINI

UNIVERSITY OF OKLAHOMA AND EUROPEAN SOUTHERN OBSERVATORY

Ego Sum ergo Mundus Est

Knowledge on the distribution of visible matter is, and has been, one of the first tasks of the astronomer. Our physical horizon has expanded with time in parallel with the development of new technology and deeper understanding of the observations.

Around the third decade of this century the development of the theory of relativity and the work by Hubble on the expansion of the Universe started considerable work on homogeneous world models. Clustering of galaxies was, for quite a while, unessential to the discussion of world models partly because in the work of Hubble there was no strong evidence that this was in fact a general phenomenon in the distribution of matter. Observationally the main goal had become the determination of the Hubble constant and of the deceleration parameter from the Hubble relation between redshift and magnitudes. In recent years however, thanks to a wealth of observational material and its interpretation, there has been a considerable revival of interest in the large-scale mass distribution and on what it might tell us about the nature and evolution of the Universe. As Peebles has said, the great excitement in current cosmology is that we have opened an observational and theoretical window in the world of mathematical models and we are now looking in them, confronting them with the observations with the feeling that the prospects are excellent to understand some of the details of the grand design of nature.

These lectures deal with the distribution of galaxies and with the characteristics of the large scale structures (size 50-100 Mpc). Intergalactic dust is not taken into account since the information we have on it is very scanty. Equally missing are observational data on the distribution of the gas over large scales. These lectures are not complete in the sense that it is not my plan to review the work in the field but rather focus on some observational aspects of the problem, which I believe to be of some interest and in which I have been somewhat involved. I have also avoided discussing the superb and fundamental theoretical work accomplished in the field.

I - THE OBSERVATIONS

One of the first important steps in understanding the cosmos is taken by recognizing, counting, and interpreting the distribution of those objects which may be the markers of the distribution of matter. Milestones toward our present understanding have been:

HUBBLE: The counts of galaxies made by Hubble (1934), using the 100 inch telescope at Mt. Wilson gave him evidence of a Universe dominated by a homogeneous distribution of galaxies. Clustering was not a very common phenomenon. Figure 1 shows the distribution of galaxies and the zone of avoidance due to the absorption near the galactic plane.

SHAPLEY: Shapley was the first one to call attention to clustering of galaxies on a very large scale. His work in collaboration with Ames (1932), gave evidence of the existence of the local Supercluster, figure 2, and of other structure which were detected both in the northern and southern hemisphere, figure 3. de Vaucouleurs' studies (Vaucouleurs, 1956) clarified some of the characteristics of the local supercluster. The catalogues of other regions of the sky published by Shapley are of a more limited usefulness because of inaccuracies in the magnitudes and, at faint magnitudes, misidentification of galaxies. They are, however, useful in planning observations and estimating the galaxian distribution. These are especially useful for the southern sky.

The correlation between Shapley magnitudes and B magnitude for galaxies in the region is illustrated in figure 4.

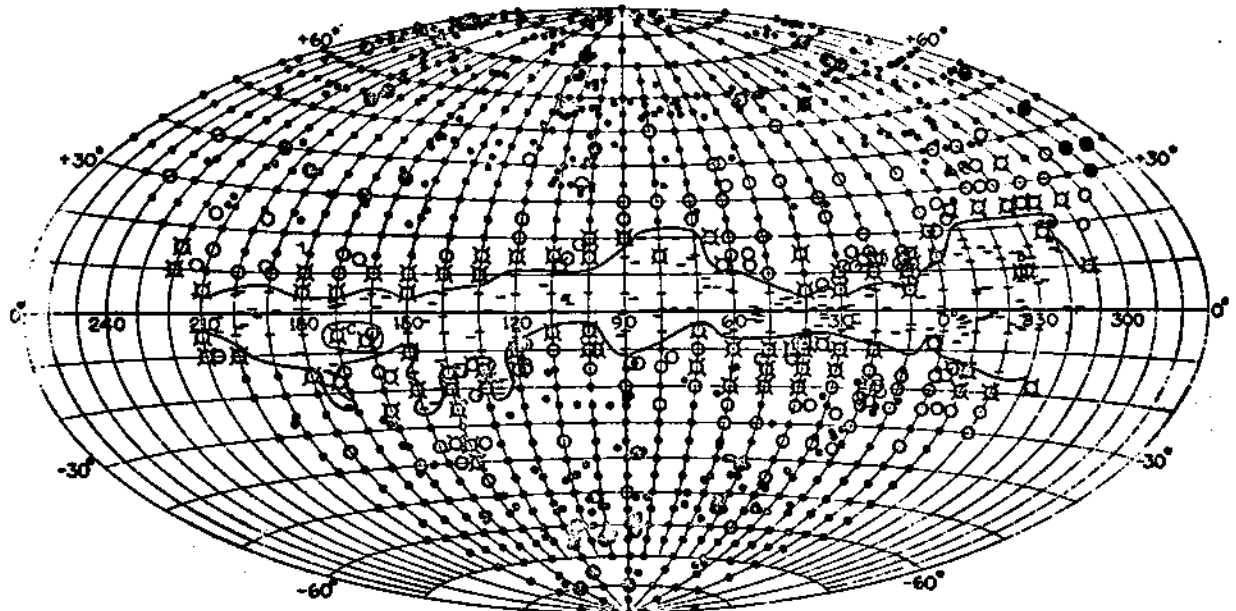


FIGURE 1 - Hubble's illustration of the region of avoidance, based on photographs taken with the Mount Wilson reflectors.

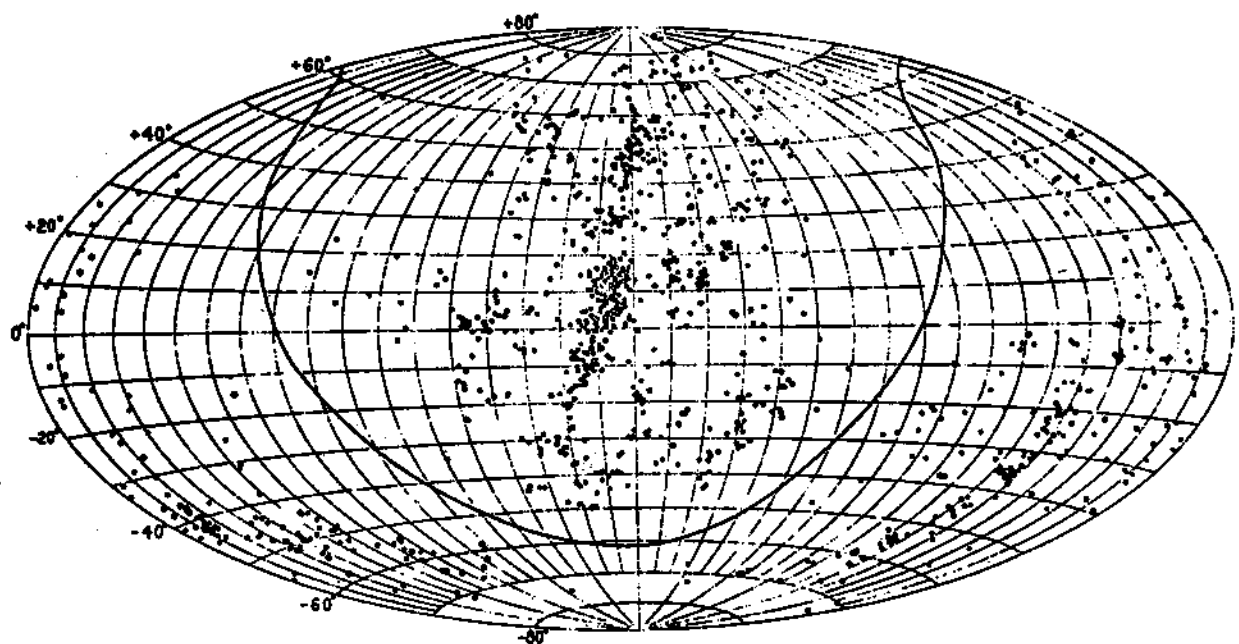


FIGURE 2 - The distribution of the extragalactic nebulae brighter than the 13th photographic magnitude. The 291 nebulae brighter than the 12th magnitude are shown by open circles; dots represent the 734 nebulae between the 12th and 13th magnitudes. The central line of the Milky Ray is indicated

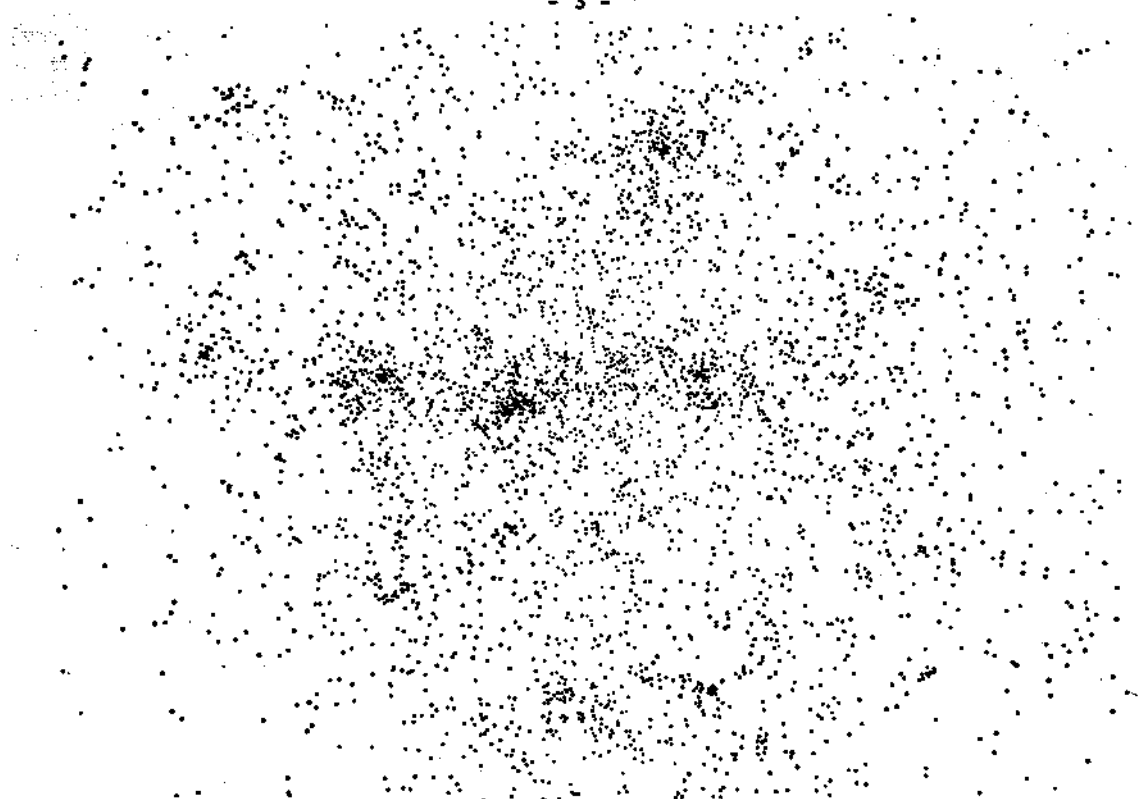


FIGURE 3 - This plot, made from a 3-hour-exposure photograph with the Bruce doublet at the Boyden Station, shows the distribution of 4000 galaxies heretofore unrecorded. The field center is at R.A. 13h 25m, Dec. - 31°.

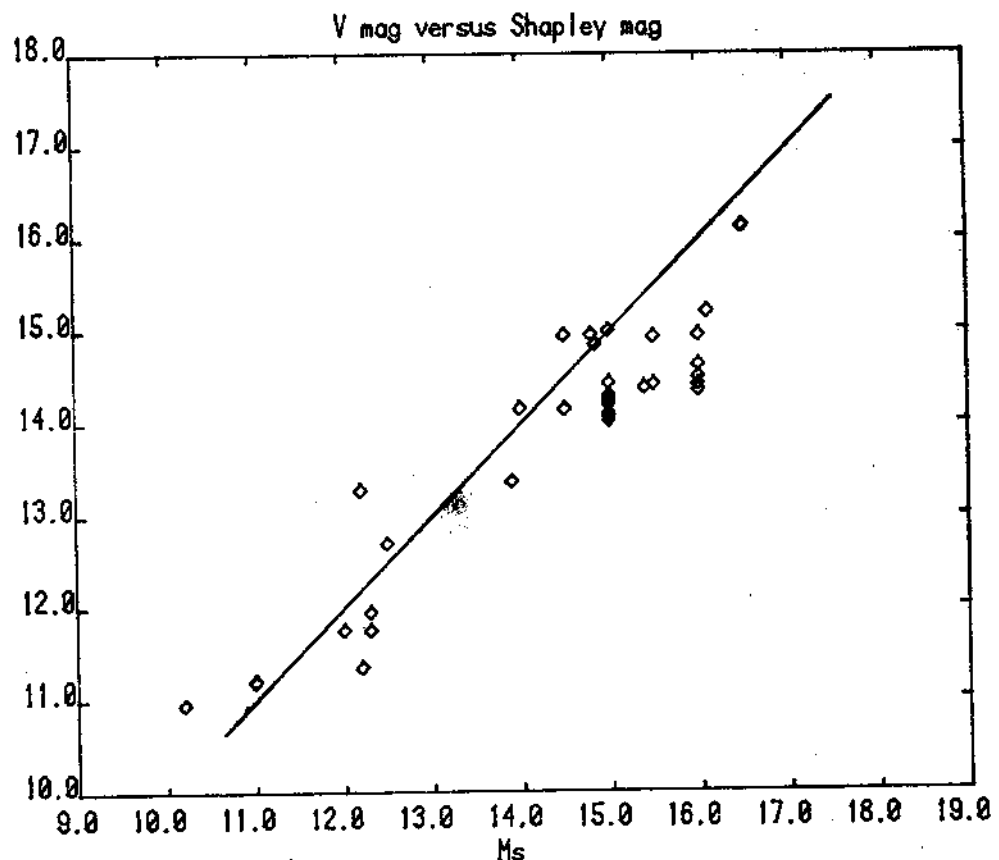


FIGURE 4 - Correlation between V magnitudes (32 arcsec diaphragm) and Shapley Magnitudes. The graph is only indicative since I have used only part of our observations. The correlation is fairly good for magnitudes brighter than $m_s = 15.0$. The continuous line is only for reference, $m_s = V$.

ZWICKY: Zwicky (1970) was convinced that clusters are the unit cells of the Universe. According to him superclustering, or II order clustering in the sense of a cluster of clusters of galaxies similar to the way we think of Coma as a relaxed cluster of galaxies, does not exist. In figure 5 I reproduce a sketch made by Zwicky in 1970 in which is contained his basic idea, at that time, on the distribution of matter. Clusters are generally very large, tenously connected to one another and superimposed on a uniform back-ground. Zwicky always insisted that according to his observations with the 18 inch Schmidt telescope the Coma cluster had to be much larger than generally accepted, see also Morphological Astronomy (1957). Zwicky and his collaborators gave to astronomy a fundamental catalogue of galaxies and clusters of galaxies (Zwicky, F. et al., 1961). A southern-extension to fainter and more accurate magnitudes is in progress by Jones

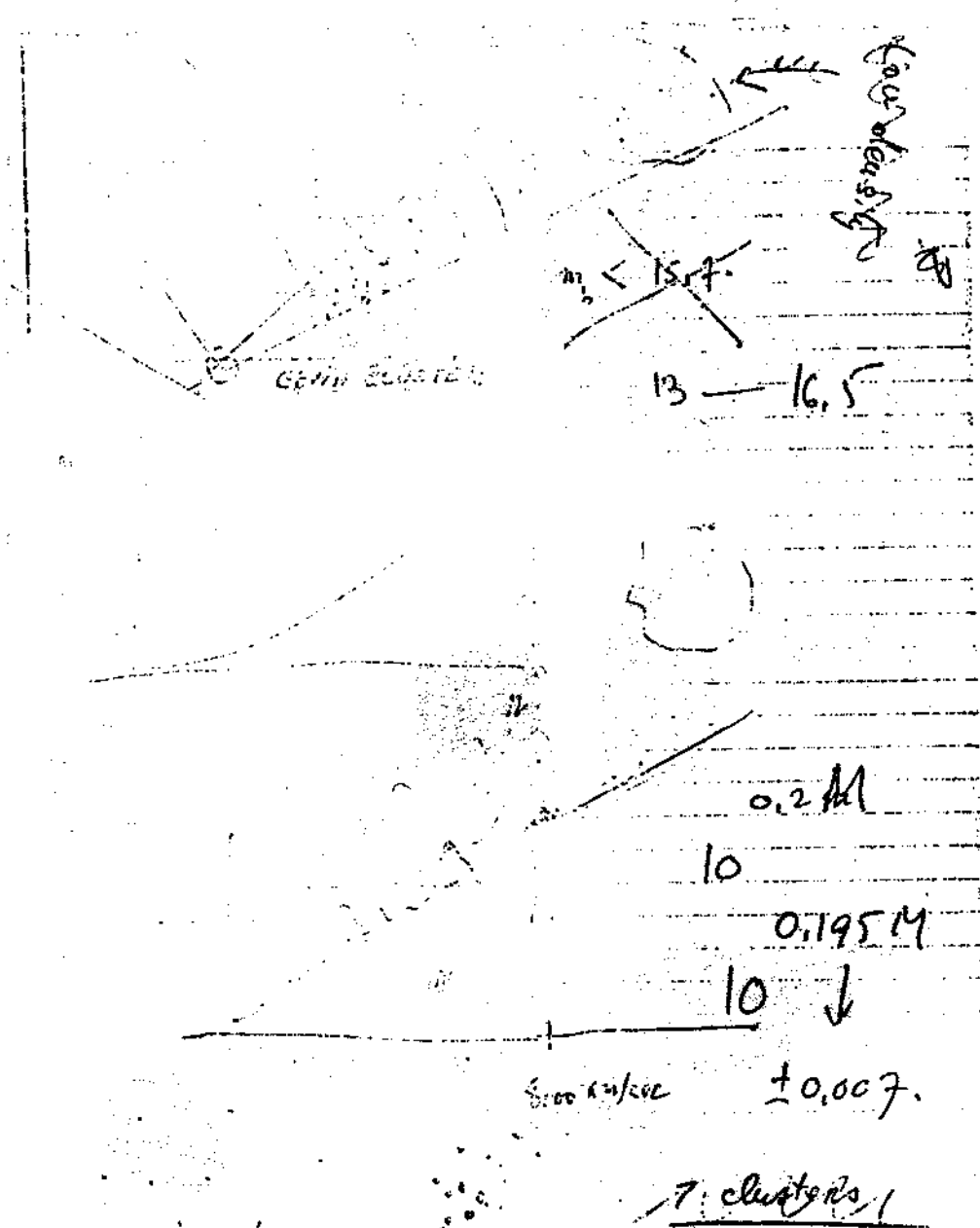


FIGURE 5 - The lower part of the figure shows how, in Zwicky's conception, there is continuity of galaxies among clusters. Clusters are super-imposed to a uniform background. The redshift refers to the distance of Coma (Coma is actually at $\langle V_0 \rangle = 6950 \text{ km/sec}$).

ABELL: Abell investigated the distribution of clusters, and their characteristics, on the POSS. His catalogue (Abell, 1958) lists 2712 (*) clusters and his analysis not only shows that clustering is a very common phenomenon, but also that the distribution of clusters is not random, figure 6. The three plots refer, from bottom to top, to clusters of increasing distance class. The characteristic cell size (maximum deviation from randomness) in degrees decreases, as expected with distance. The southern extension of the catalogue, based on the U.K./E.S.O. survey is at the present under completion.

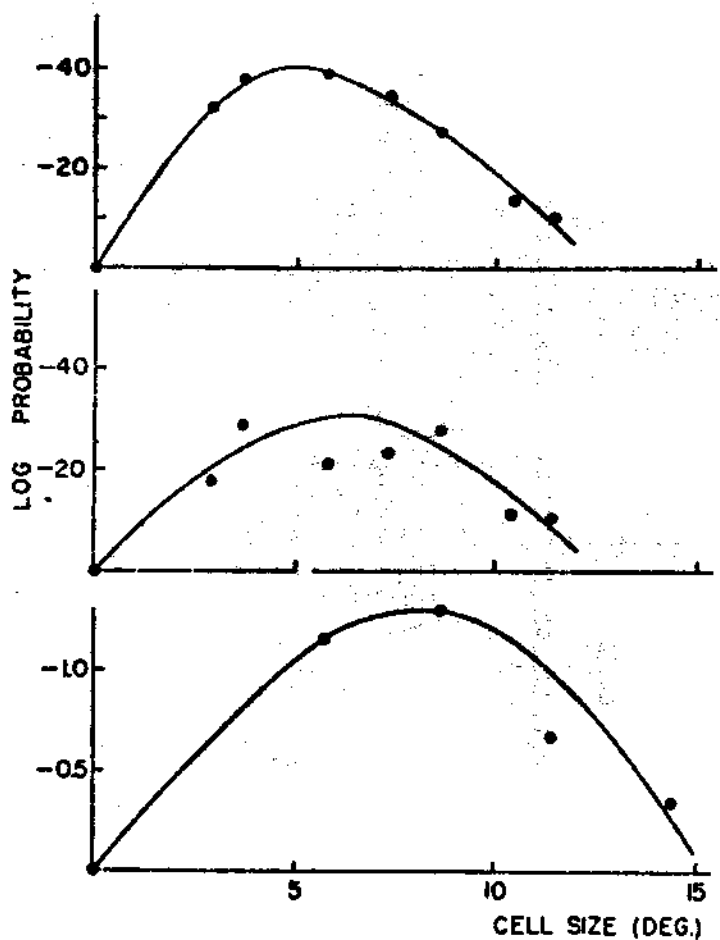


FIGURE 6 - Probabilities that the observed frequency distributions of clusters among cells of various sizes would be obtained in random samplings from populations distributed with a Poisson law.

In the Zwicky catalogue the Virgo-Serpens cloud coincides with field N.49 where a grouping of galaxies at about the same magnitude of the Hercules galaxies is clearly visible. Some spectroscopic evidence exists that the galaxies in this region are at the redshift of Hercules (10500 km/sec), Shane and Wirtanen, (1954). Hopefully soon a complete redshift sample of galaxies in this region, which for some years has been eluding us, will be available.

Observations by Giovanelli and Haynes (1982) show that a large number of galaxies in this region are indeed at the redshift of the Hercules supercluster.

SHANE: Shane and his collaborator Wirtanen undertook and completed a fundamental work on the distribution of galaxies. A large part of the northern sky was surveyed using the Lick 20-inch double astrograph, and galaxies were counted down to about the 19.0th magnitude in cells with a resolution of 10 minutes of arc (the published counts (Shane et al., 1967) have a resolution of 1 degree x 1 degree).

The work is very accurate. Shane and Wirtanen recognized the presence of structures larger than clusters, figure 7, which they called clouds of galaxies. The Hercules cloud described by Shane and Wirtanen has been studied by Tarenghi et al. and is discussed later in these lectures. There is now evidence that such structure extends toward the north and is somehow connected to the clusters A2197/99. Quite probably the supercluster extends further south and is connected to the cloud Serpens Virgo (I use here the Shane and Wirtanen nomenclature), figure 8.

(*) 1682 of these clusters form a homogeneous subsample.

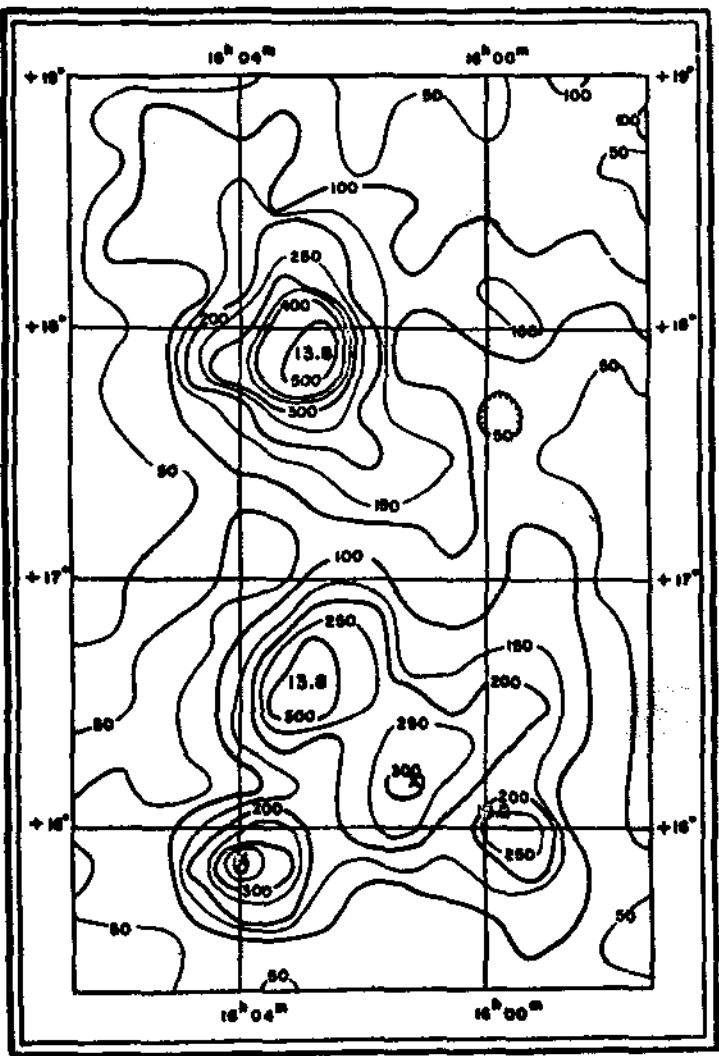


FIGURE 7 - The density enhancements in the Hercules cloud correspond to the clusters A2151, A2147 and A2152.

framework of cosmology and the formation and growth of perturbations which should evolve in the structured distribution we observe at the present time. Independent of the cosmological model this type of analysis is a valid tool to compare the observations with theories. Such analysis was applied to the Shane and Wirtanen counts of galaxies by Totsuji and Kihara(1969) also.

The probability of finding a galaxy in an element of volume dV is given by

$$dp = \langle n \rangle dV \quad (1)$$

where $\langle n \rangle$ is the mean number density. If we consider two volume elements dV_1 , and dV_2 , the joint probability of finding a particle in each element can be defined as

$$dp = \langle n \rangle^2 [1 + \xi(R_1, R_2)] dV_1 dV_2 \quad (2)$$

where $\xi(R_1, R_2)$ is a two point correlation function defined in the range $-1 \leq \xi \leq +\infty$. A random

Vorontsov-Velyaminov catalogued galaxies and gave detailed information on the single objects. Such a catalogue is of limited usefulness for statistical studies. The deepest survey has been made by Rudnicki et al. (1973) in a 6×6 field, the Jagellonian catalog.

Naturally our knowledge of the distribution of galaxies is greatly enhanced if we can add to the space distribution the third dimension, redshift. This is possible because on a large scale (or distance) the doppler shift caused by the peculiar position of galaxies, outside clusters, is small compared to the cosmological redshift. The development of sensitive multichannel detectors allowed the undertaking of such observational programs during the seventies. The development of spectrographs with the capability of observing a set of objects simultaneously (Geyer, 1979; Angel, 1980) will largely increase our knowledge of the Universe at large distances.

THE AUTOCORRELATION FUNCTION

The two dimension (surface) distribution of galaxies, and especially the accurate counts by Shane and Wirtanen, has been analyzed by various astronomers using sophisticated statistical methods. Among those of remarkable interest are the studies by Neymann et al.(1953) and by Peebles and his collaborators (1980). The latter extensively developed the autocorrelation analysis and its interpretation in the

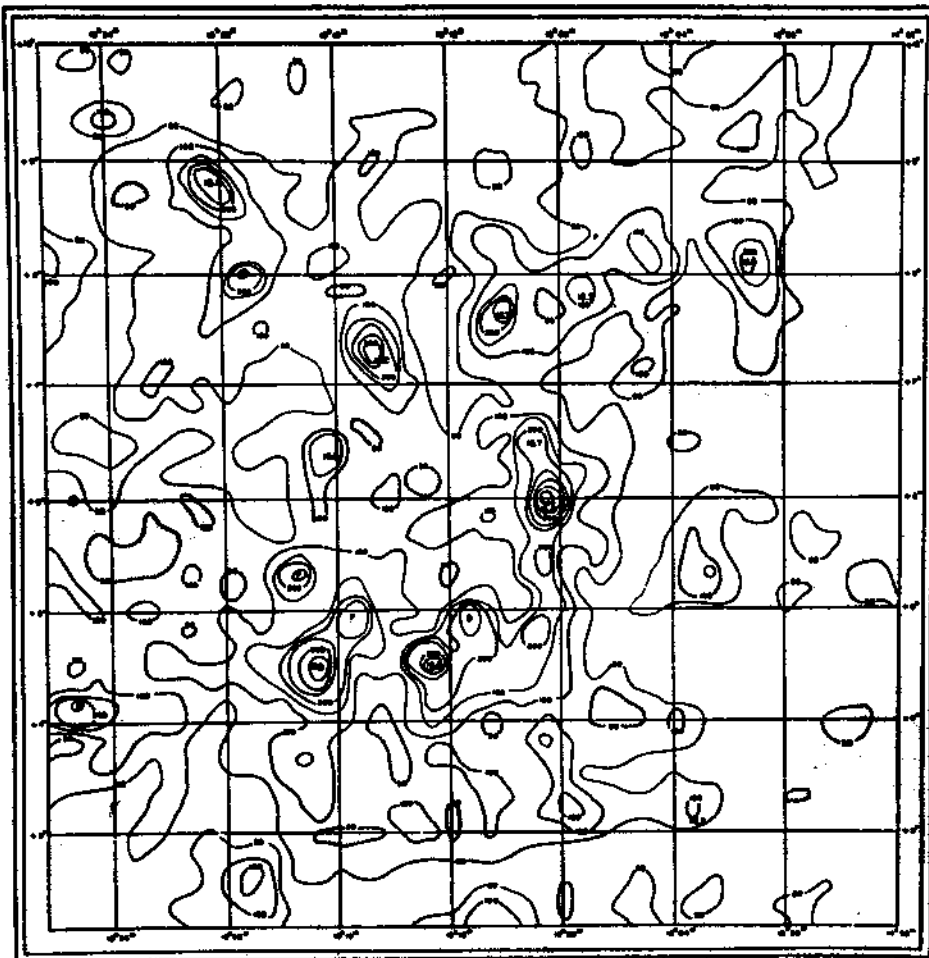


FIGURE 8 - The Serpens-Virgo cloud. A spectrum obtained long ago by Mayall gave the first indication that such structure may be at the distance of the Hercules Supercluster.

Poisson distribution of points is described by the autocorrelation function $\xi = 0$.

A positive value of the function defined by equation (2) implies clustering while a negative value implies antoclustering. Given one particle, the probability in excess of the random probability ($dP = \langle n \rangle dV$) of finding another particle located at a distance r and within the volume element dV is dP (in excess of random) = $\langle n \rangle \xi(R)dV$. Therefore the probability of finding a particle at a distance R from another particle and within a volume element dV is given by

$$dP = \langle n \rangle [1 + \xi(R)]dV \quad (3)$$

These concepts can be easily generalized for density distributions in continuous fluids.

If galaxies are in clusters of diameters D_{cl} and clusters are distributed randomly in space we would expect an autocorrelation function which is positive for $R < D_{cl}$ and $\xi(R) = 0.0$ for $R > D_{cl}$. If we choose a galaxy at random, in fact, we have a probability greater than random (equation (3)) of finding another galaxy at a distance $R < D_{cl}$. However if $R > D_{cl}$ the second galaxy belongs to another cluster which is randomly distributed with respect to the first cluster (of which the first galaxy is a member). Therefore $\xi(R) = 0$. The shape of the function will depend on the cluster density profile. For a more detailed example see Appendix 1.

The mean number of neighbors within a distance R of a randomly chosen object, is:

$$\langle N \rangle = \int \langle n \rangle V [1 + \xi(R)] dV = \langle n \rangle 4\pi/3 R^3 + \langle n \rangle \int \xi(R) dV \quad (4)$$

and the total number of neighbors in excess of random is:

$$N_c = 1 = \langle n \rangle / \int \xi dV \quad (5)$$

so that, if the integral converges, N_c is one measure of the mean number of objects per cluster. For a statistical determination of physical parameters and further details see Peebles (1980) and references therein.

THE LUMINOSITY FUNCTION

We have some evidence that the luminosity function of galaxies has, at least in the first approximation, the same functional shape for galaxies which are in clusters and for galaxies which are outside of clusters. The function represents the relative number of galaxies of different absolute luminosities or, in other words, the number of galaxies per Mpc^3 with absolute magnitudes between M and $M + dM$. A convenient form has been proposed by Abell (1962) for the Coma cluster:

$$n(<M) = Adex (\alpha M); \quad \alpha = 0.75; \quad M < M' \quad (6)$$

$$n(>M) = Bdex (\beta M); \quad \beta = 0.25; \quad M > M' \quad (7)$$

where $n(<M)$ is the number of galaxies per unit volume which are brighter than the absolute magnitude M and A, B must satisfy the condition of continuity

$$Adex (\alpha M') = Bdex (\beta M') \quad (8)$$

We can write, therefore, the above equation in the following form:

$$n(<M) = Cdex \left[\beta(M - M') \right]; \quad M > M' \quad (9)$$

$$n(<M) = Cdex \left[\alpha(M - M') \right]; \quad M_0 < M < M' \quad (10)$$

$$n(<M) = 0; \quad M < M_0 \quad (11)$$

where $C = Adex (\alpha M')$; M_0 is the absolute magnitude of the brightest galaxy and

$$M' = -18.6 + 5 \log h \quad (h = H/100). \quad (12)$$

Recently Schechter (1976) parametrized the luminosity function in a form which is very convenient for computation. He has shown that the observational data are equally well fitted by the equation (differential luminosity function):

$$\phi(L)dL = \phi'(L/L')^\alpha \exp(-1/L')d(L/L') \quad (13)$$

or expressed in magnitudes:

$$\phi(M)dM = Kdex(-0.4(M-M'))(\alpha+1)\exp(-dex(-0.4(M-M')))dM \quad (14)$$

where

$$\alpha = -1.25; \quad L' = 3.4 \cdot 10^{10} L_B; \quad M_B' = -20.6$$

and K and ϕ' are normalization constants. The luminosity function for field galaxies is illustrated in figure 9, Felten (1977). Some useful relations are given in appendix 2.

The above concepts are very useful in the analysis and preparation of the observations. For statistical purposes it is convenient to select samples which are complete to a limiting magnitude which is generally selected as the best compromise between practical constraints: equipment and telescope time available, and research goals. The observational sample is therefore characterized by a selection or completeness function of the Fermi type

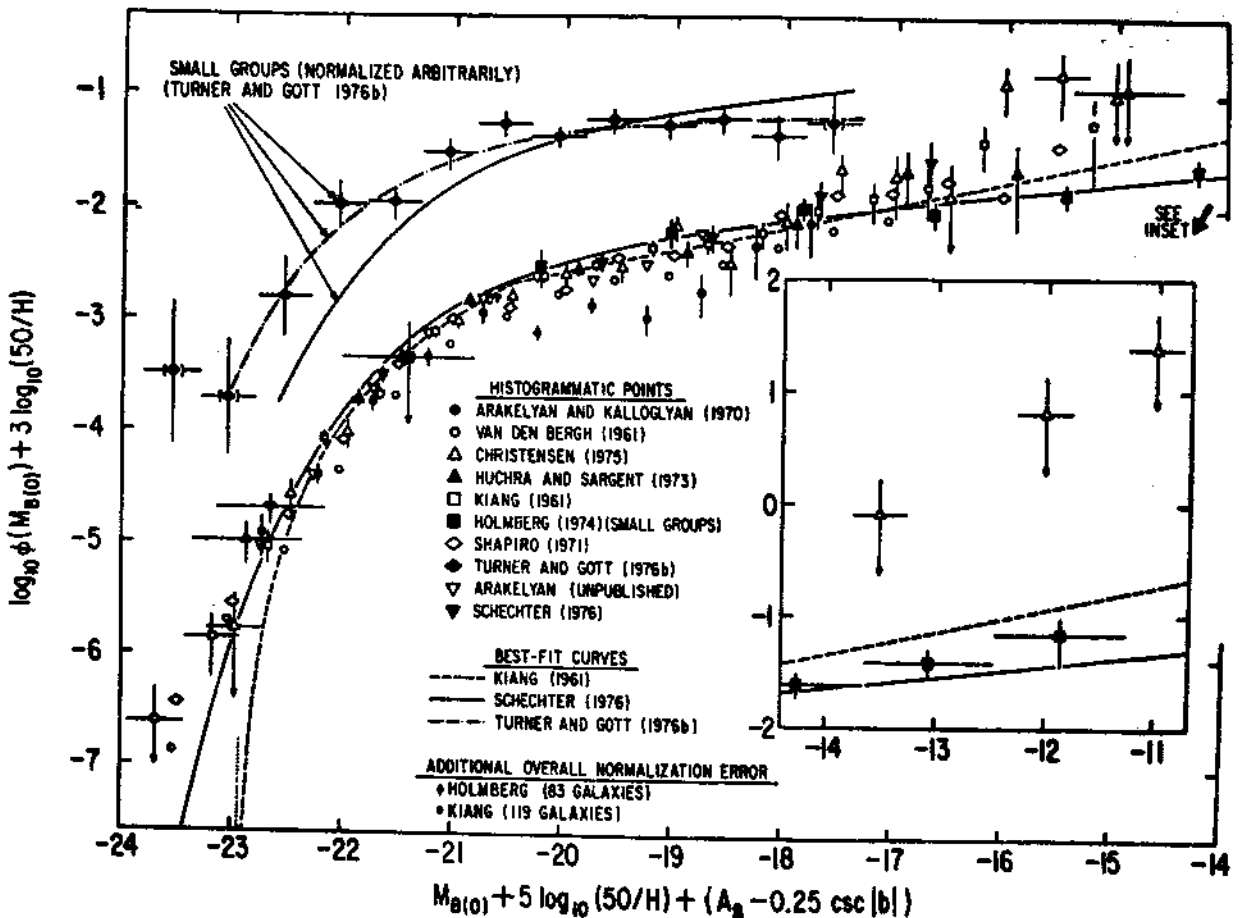


FIGURE 9 - The luminosity function for field (non-cluster) galaxies (Falten, 1977).

$$f(m) = \left\{ \exp \left[(m - m_1)/\Delta m_1 \right] + 1 \right\}^{-1} \quad (15)$$

An approximation often used, however, is the step function, $f(m) = 1$ for $m < m_1$ and $f(m) = 0$ for $m > m_1 (\Delta m_1 + 0.0)$.

II - RESULTS FROM COUNTS OF GALAXIES

From the observations we can determine the two particle angular correlation function, $w(\theta)$ and if the luminosity function of galaxies is known, it is possible to relate $w(\theta)$ to $\xi(R)$. A full derivation of the relation between $w(\theta)$ and $\xi(R)$ can be found in Peebles (1980). Approximating the observed function $w(\theta)$ by a power law of the form $w(\theta) = A \theta^{-\delta}$ where $\delta = 0.77 \pm 0.04$, figure 10a, b, the autocorrelation function is given by the power law:

$$\xi(R) \propto (R/R_0)^{-\gamma} \quad (16)$$

with $\gamma = \delta + 1 = 1.77 \pm 0.04$ and $R_0 = 4.23 \pm 0.26 h^{-1} \text{ Mpc}$.

There is no a priori reason for choosing a power law to fit the observations, but a power law seems to be sufficient in view of the uncertainties in the data. Equation (9) quantifies, to some extent, what was first noticed by Zwicky (1957) and Shapley; galaxy clustering is a very pronounced effect. It tells us that the most probable location for a galaxy is near another galaxy. This type of analysis is very interesting due to various built in properties. The power law is a reasonable fit from the size of individual galaxies to the size of super-clusters of galaxies. This may suggest a common mechanism which should explain the formation of clusters on various scales. Since the autocorrelation is unrelated to a reference position it tells us about characteristic lengths of structures which are homogeneously distributed.

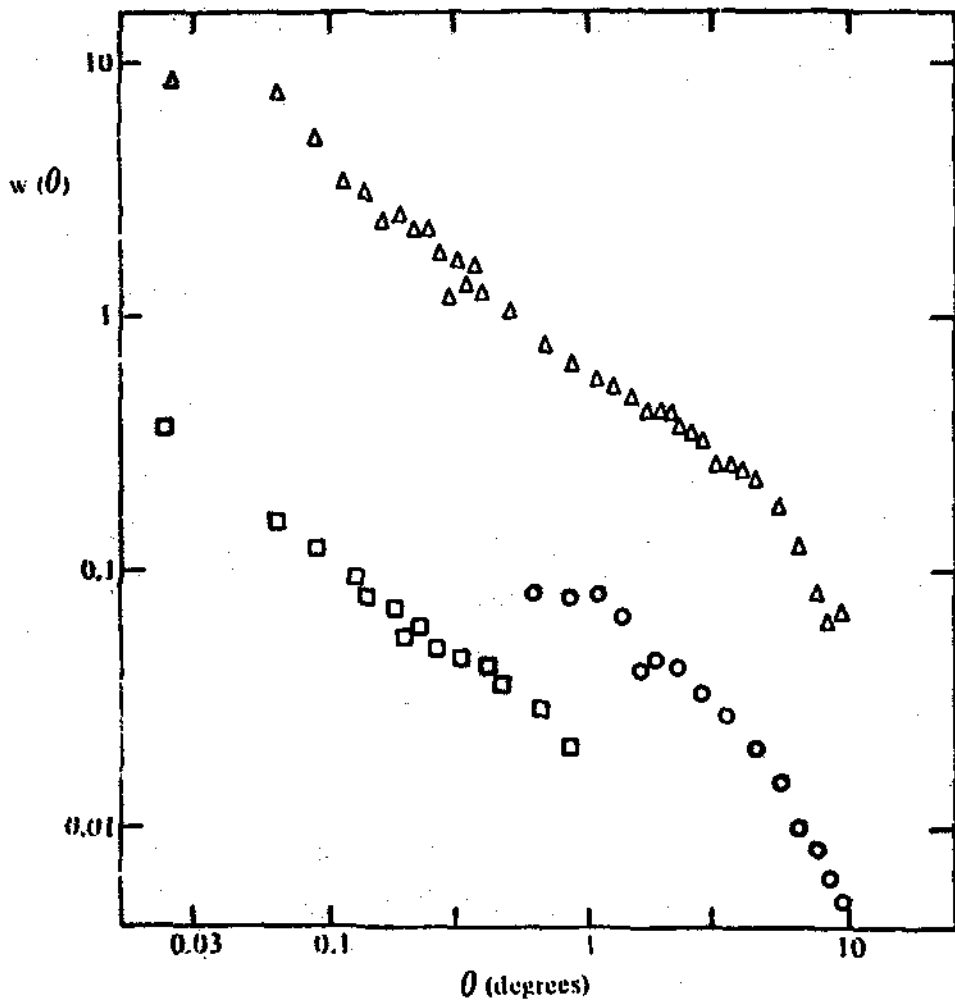


FIGURE 10.A - Correlation functions for various catalogs of galaxies (from Peebles, 1975): Jagellonian (squares), Zwicky (triangles) and Shane-Wirtanen (circles).

In other words the homogeneity of the Universe at large scales is contained in the results.

Another remarkable result is that the function seems not to have bumps or shoulders. This is in agreement with the fact that the clustering of matter does not show sharp edges but rather a smooth slope and structures of various types may be connected among them by regions of very low density. A set of characteristic sizes cannot be defined.

Finally, the slope of the correlation function today must be related to the formation of the observed structures, that is it must be related to the spectrum of the initial density perturbations in the early Universe. Since perturbations grow at different rates in different cosmological models, the study of the large scale structures through the autocorrelation function or their detailed characteristics may be a very good test of cosmological models.

Counts of galaxies can give us only limited, and model dependent, information on the three-dimensional distribution of galaxies. At very large radii, of the order of 20 h Mpc, the analysis must be seriously limited by noise so that no information can be gained on the very large structures.

The powerful tool of the statistical analysis can not give us information on the detailed structure of clustering. Such information needs to complement the statistical studies and may be of primary importance in the understanding of the distribution of mass on a large scale and enable additional tests on cosmological models.

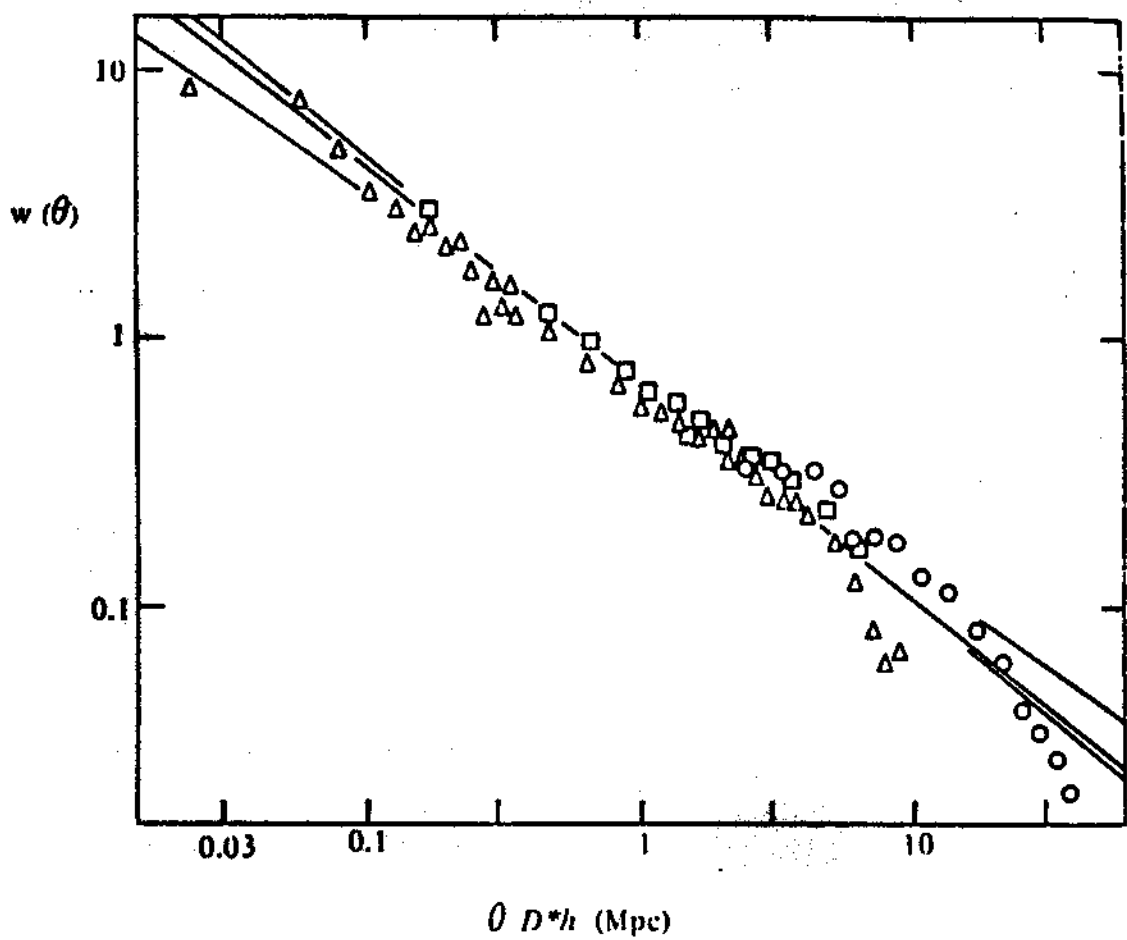


FIGURE 10.B - The correlation functions after scaling for the different depth of the surveys.

III - THE DISTRIBUTION OF GALAXIES, REDSHIFTS

The only way to understand nature is to observe it. Of course we have the non-trivial task to interpret and understand what we observe.

Observations of redshifts of large samples of galaxies became feasible, using a reasonable amount of telescope time, toward the end of the sixties after the introduction of commercially made image tubes. At that time Rood and I, encouraged by T. Page, were interested in understanding the size of the Coma cluster, a problem which puzzled Zwicky since the time he observed this region with the 18-inch Schmidt telescope on Mount Palomar. This work developed our interest in the large scale structure especially after we discussed our results with Peebles and Oort. A posteriori it is clear that a better knowledge of the literature, of the theoretical work, and above all of the work of Shapley, Shane and Wirtanen and others, was calling for surveys in redshifts, a need often stressed by Zwicky (1957) and Mayall (1960).

If we observe a sample of galaxies complete to a chosen limiting magnitude and assume a homogeneous distribution of objects we can derive the expected distribution of redshifts, Chincarini (1978). The number of galaxies in the solid angle $\Delta\Omega$ with velocities in the range (V_i, V_j) and apparent magnitudes brighter than m_0 is given by:

$$N(V_i, V_j) = \Delta\Omega \int_{V_i/H}^{V_j/H} x^2 \phi(x) dx \quad (17)$$

where

$$x = V/H; \quad \phi(x) = f \left[M = m_0 + 5 \log \left(x/M_{pc} \right) - 25 \right]$$

and

$$f(M) = Adex \left[\beta(M - M^*) \right], \quad M \geq M^*$$

$$f(M) = Adex \left[\alpha(M - M^*) \right], \quad (M \leq M^*)$$

$$M^* = -18.6 + 5 \log (H/100); \quad \alpha = 0.75; \quad \beta = 0.25$$

If we define a characteristic distance

$$D^* = dex \left[0.2 (m_0 - M^*) - 5 \right] \text{ Mpc} \quad (18)$$

and $V^* = HD^*$ we derive the following equations:

For $V_i < V_j < V^*$

$$N(V_i, V_j) = \frac{\Delta\Omega A D^*{}^3}{3 - 5\beta} \left[(V_j/V^*)^{3-5\beta} - (V_i/V^*)^{3-5\beta} \right] \quad (19)$$

For $V^* < V_i < V_j$

$$N(V_i, V_j) = \Delta\Omega A D^*{}^3 (3 - 5\alpha)^{-1} \left[(V_j/V^*)^{3-5\alpha} - (V_i/V^*)^{3-5\alpha} \right] \quad (20)$$

For $V_i < V^* < V_j$

$$N(V_i, V_j) = \Delta\Omega A D^*{}^3 \left\{ (3 - 5\beta)^{-1} \left[1 - (V_i/V^*)^{3-5\beta} \right] + (3 - 5\alpha)^{-1} \left[(V_j/V^*)^{3-5\alpha} - 1 \right] \right\} \quad (21)$$

The total number of galaxies is given by

$$N(0, \infty) = 1.90 AD^*{}^3 \Delta\Omega \quad (22)$$

and the distribution of redshifts peaks at $V = V^*$.

The observations show that the distribution in redshifts can not be fitted by the above equations and that redshifts are segregated in discontinuous sets, Chincarini and Martins (1975). The actual distribution is shown in figure 11. At a distance of about 14 degrees from the center of the Coma cluster we still find galaxies which have the redshift of Coma, however there are not objects detected between $V = 3500$ and $V = 6500$ km/sec. Large structures, super-clusters, seem to alternate with regions which are void of galaxies to the limiting magnitude we observe. We know little, however, about the distribution of faint dwarf galaxies.

The distribution of redshifts for the Coma A1367 region, figure 12, (for the data see Gregory et al, 1978, and references therein) is illustrated in Figure 13. We notice:

- a - The clusters Coma and A1367 are tenuously connected. The density of galaxies at large distances from the cluster center decreases as $\nu(R) = R^{-2.3}$, Figure 14.
- b - Two other condensations are visible at a redshift of about $V = 4500$ km/sec and $V = 2000$ km/sec. The feature at 4500 km/sec is somewhat puzzling since it seems present over a very large region of the sky, while the galaxies at a distance of 2000 km/sec are part of the local supercluster.
- c - No galaxies are observed in the range of redshifts between $V_i = 5000$ and $V_j = 6200$ km/sec.

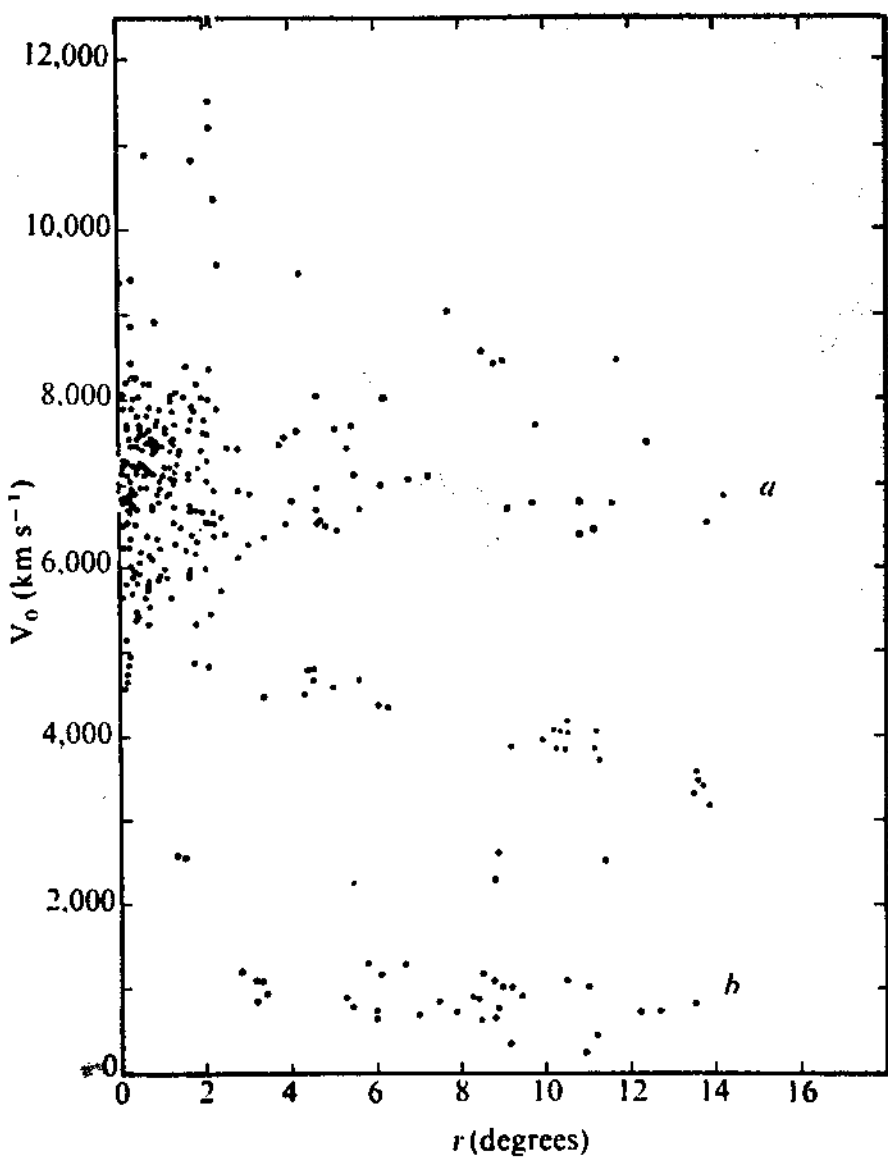


FIGURE 11 - Line of sight velocity relative to the Local Group against radial distance from the centre of the Coma cluster .

- (a) Coma cluster.
- (b) Local Supercluster.

The observed distribution of galaxies in the Hercules region, figure 15, is reproduced in figure 16. Similar features are observed in Figure 17 for the Perseus and Pisces supercluster. The distribution of Zwicky clusters for the Perseus-Pisces supercluster in two ranges of redshifts is illustrated in figure 18, Einasto et al. (1980). Finally in Figures 19 and 20 we reproduce the distribution of objects over much larger survey areas. Details are given in the captions to the figures. The indications we derive from the above observations are, as we just mentioned:

1 - Very large regions of space seem to be void of matter. While for a better understanding we may have to wait for deeper surveys, the present material tell us that if a uniform

RIGHT ASCENSION (1950)

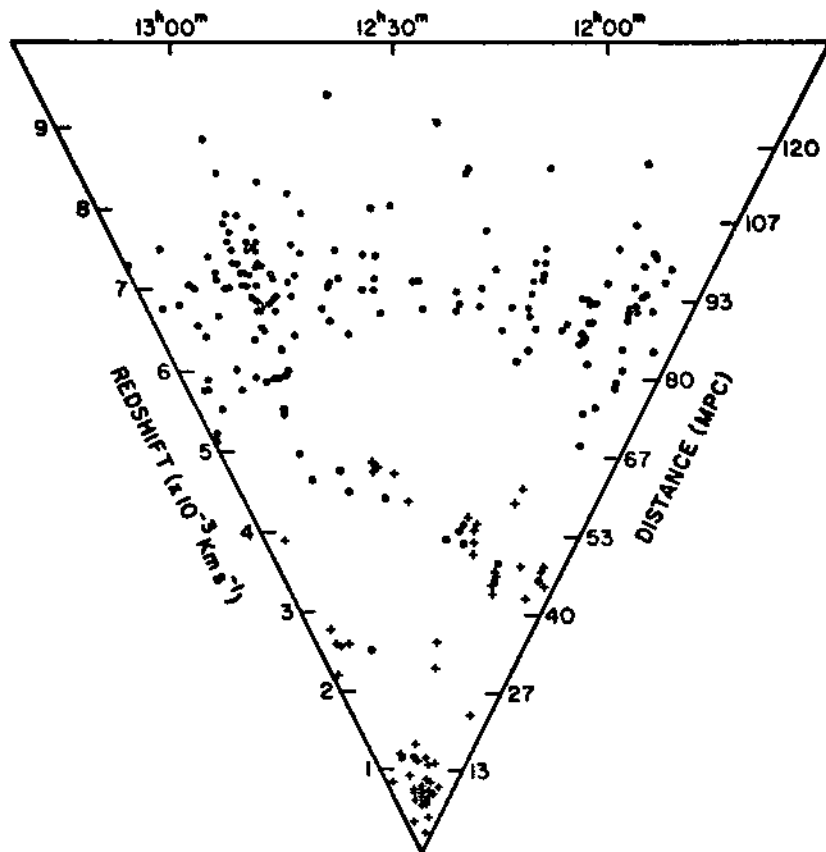
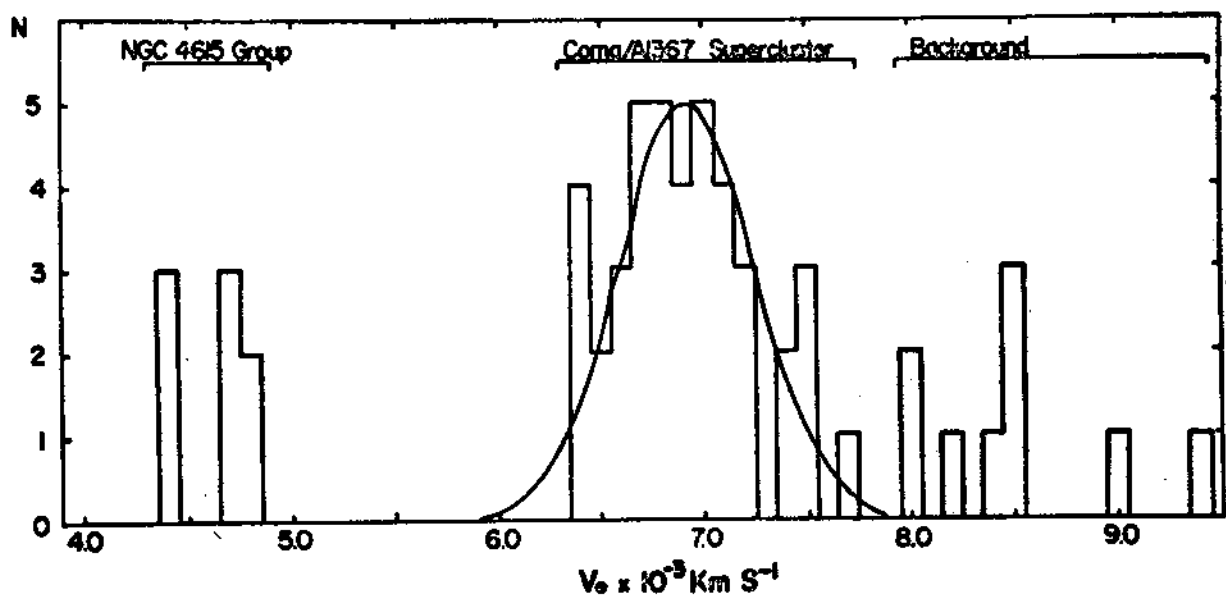


FIGURE 12 - The distribution in depth of galaxies in the Coma A1367 region. The effect of the cluster velocity dispersion is clearly visible at the R.A. of the Coma and A1367 clusters. (From Gregory and Thompson).



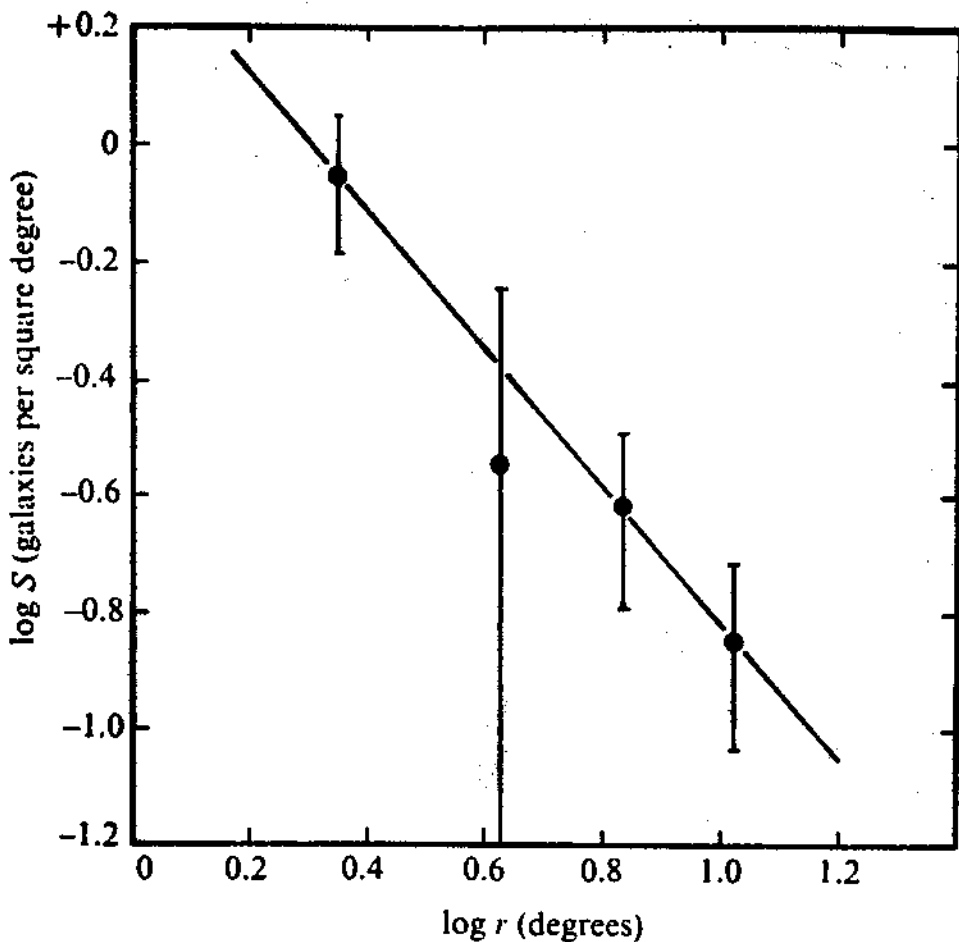


FIGURE 14 - Logarithm of the average number of galaxies in the Coma cluster with $m_p \leq 15.0$ mag per square degree against logarithm of the average radius of an annular ring. Error bars indicate the mean errors of sampling. The straight line has a slope of - 1.18.

background of visible matter exists, it is of much lower density than it was previously assumed (see Appendix 3).

2 - We detect large structures which extend over sizes of 50 to 100 Mpc. Such structures are probably interconnected and depending on how we define them, may be much larger. The explanation of such structures, their formation and evolution, may be a real challenge for theory.

3 - Clusters and groups are units which are embedded in the superclusters. Clusters are thought to be virialized.

4 - There is no evidence of higher order clustering.

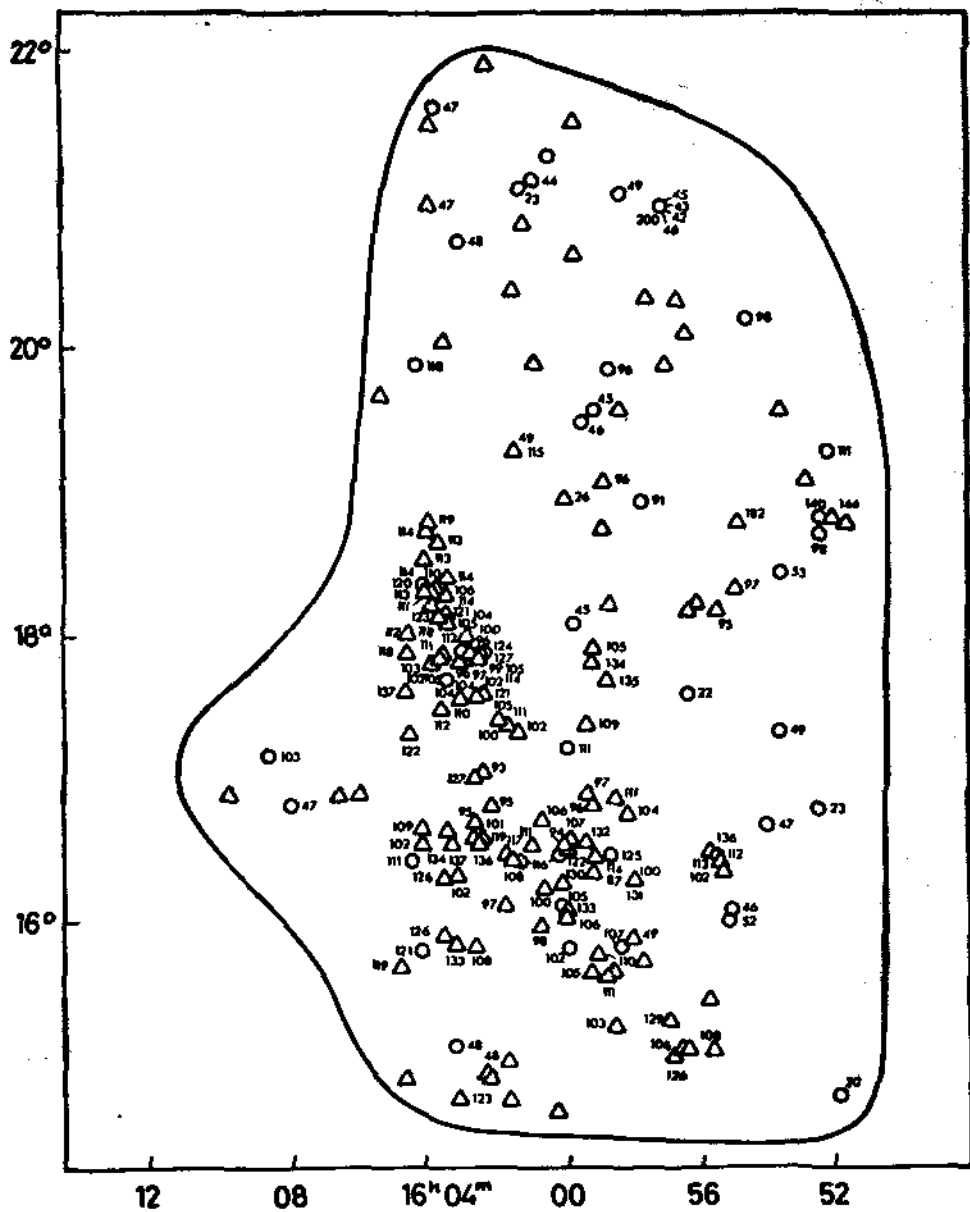


FIGURE 15 - Redshift map of the observed field of the Hercules supercluster. Redshifts in units of 100 km s^{-1} . Symbols for galaxies represent apparent magnitudes (see CGCG for key).

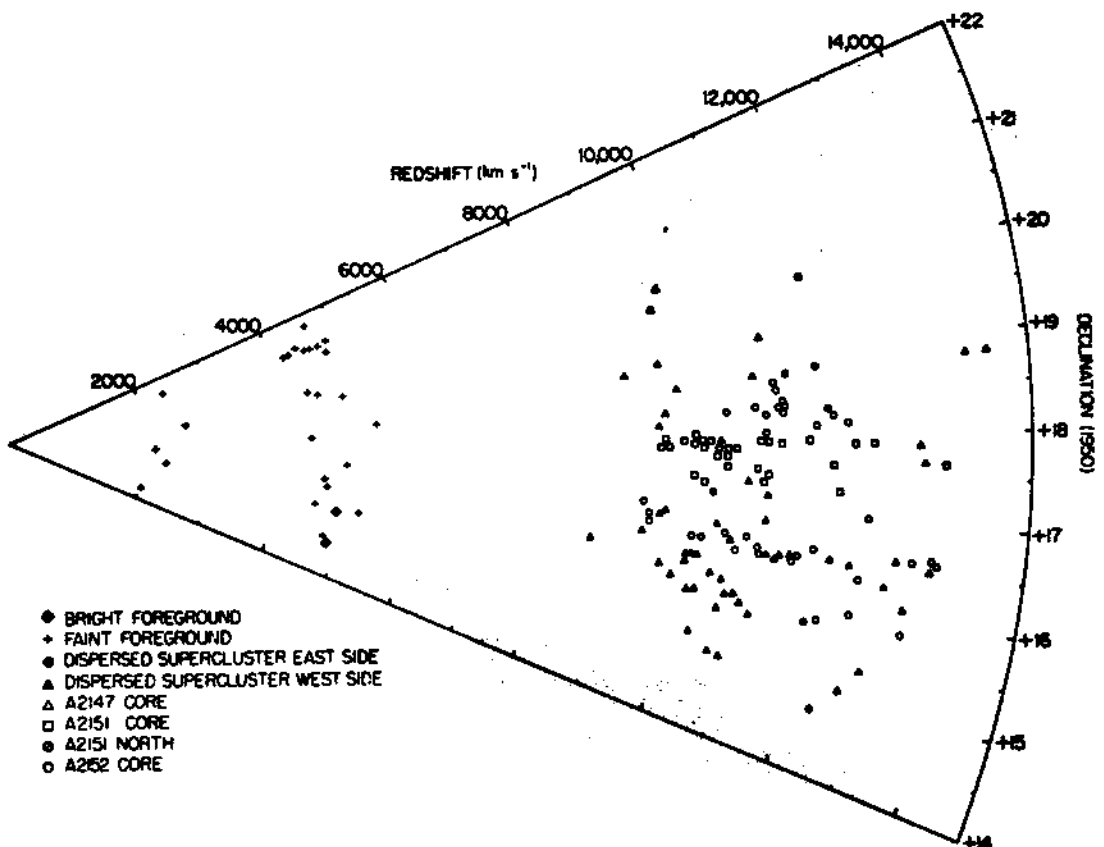


FIGURE 16 - "Cone Diagram" - redshift versus declination - for the galaxies in the observed field of the Hercules supercluster. Bright foreground galaxies are those sufficiently luminous to be in the observed sample if located at the distance of the Hercules supercluster. A2147 core and A2152 core are the galaxies within one Abell radius of the respective cluster centers. A2151 core are the galaxies within one Abell radius of the center of A2151 but with $\delta \leq 18^{\circ}0$, while A2151 North are the remaining galaxies with $\delta > 18^{\circ}0$. The galaxies beyond one Abell radius of the centers of A2147, A2152, and A2151 and with $8000 \text{ km s}^{-1} \leq V_0 \leq 15,000 \text{ km s}^{-1}$ are members of the dispersed component of the Hercules supercluster. The sample is incomplete north of $\delta = 20^{\circ}$.

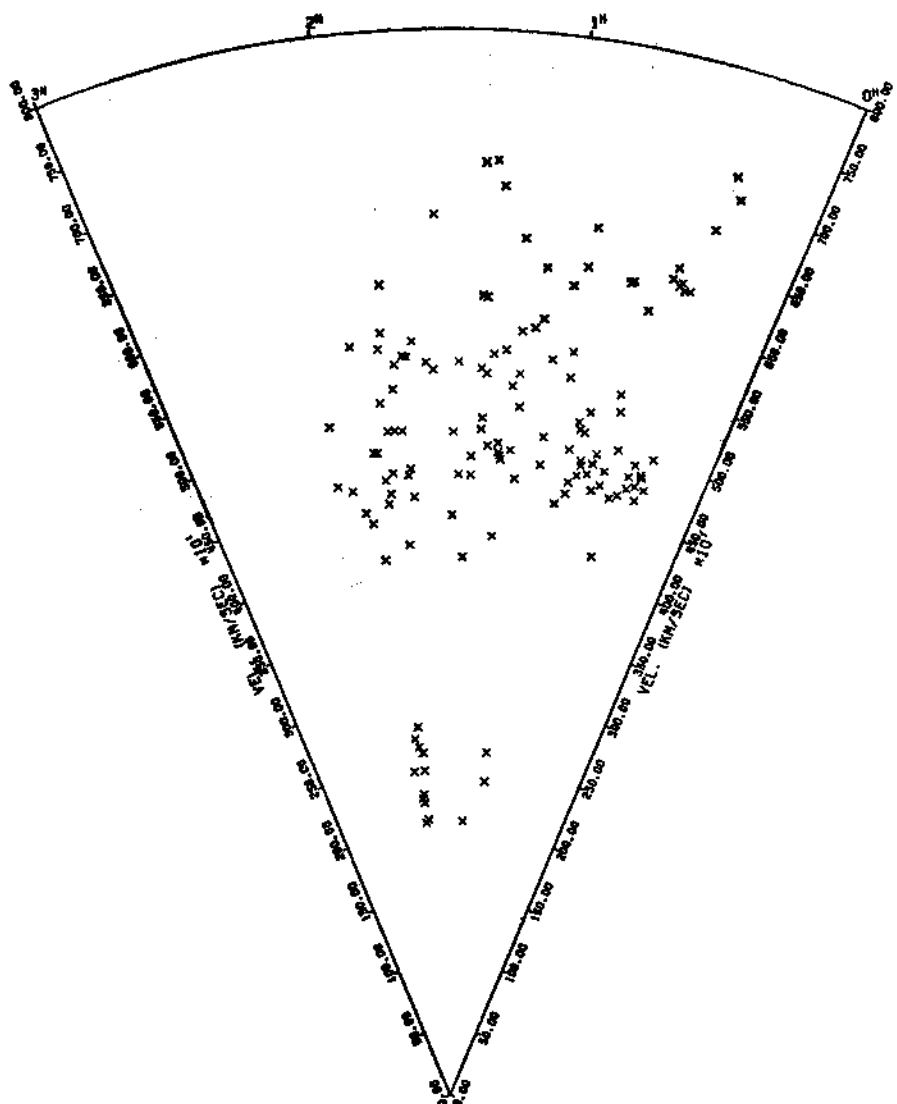


FIGURE 17 - The distribution in depth of galaxies which are part of the Perseus-Pisces super-cluster.

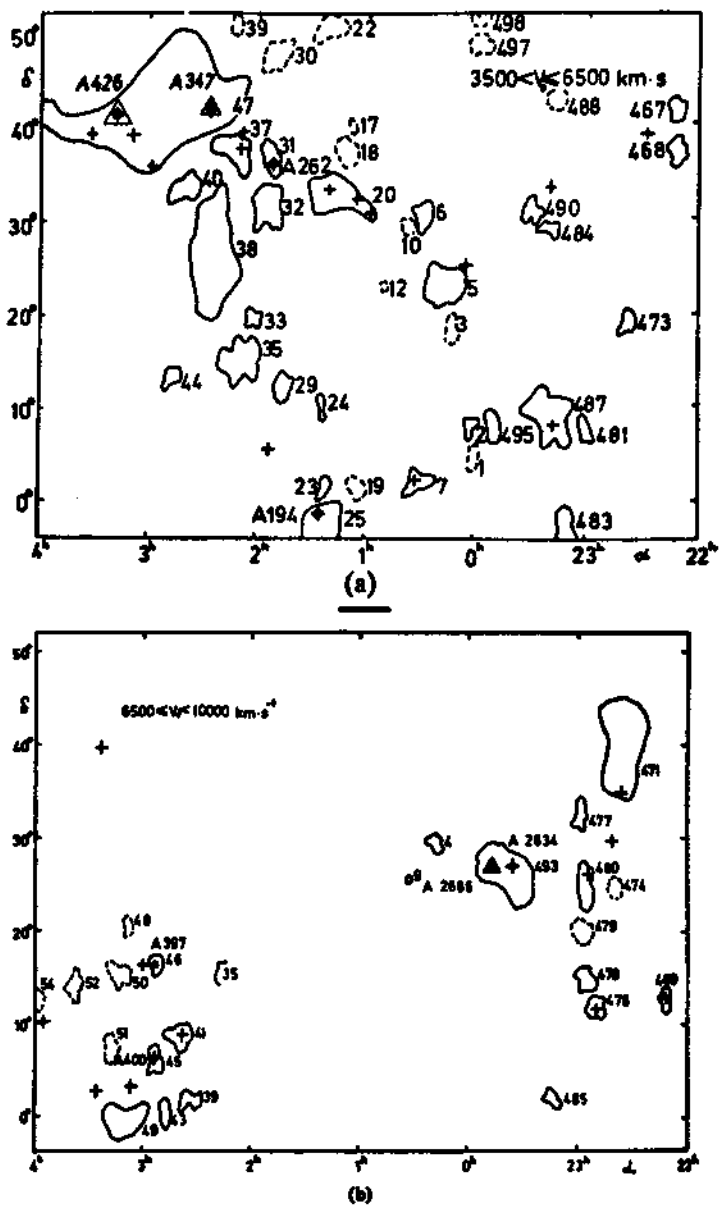


FIGURE 18 - The distribution of Zwicky-clusters in the region of the Perseus-Pisces super-cluster according to Einasto et al. (1980).

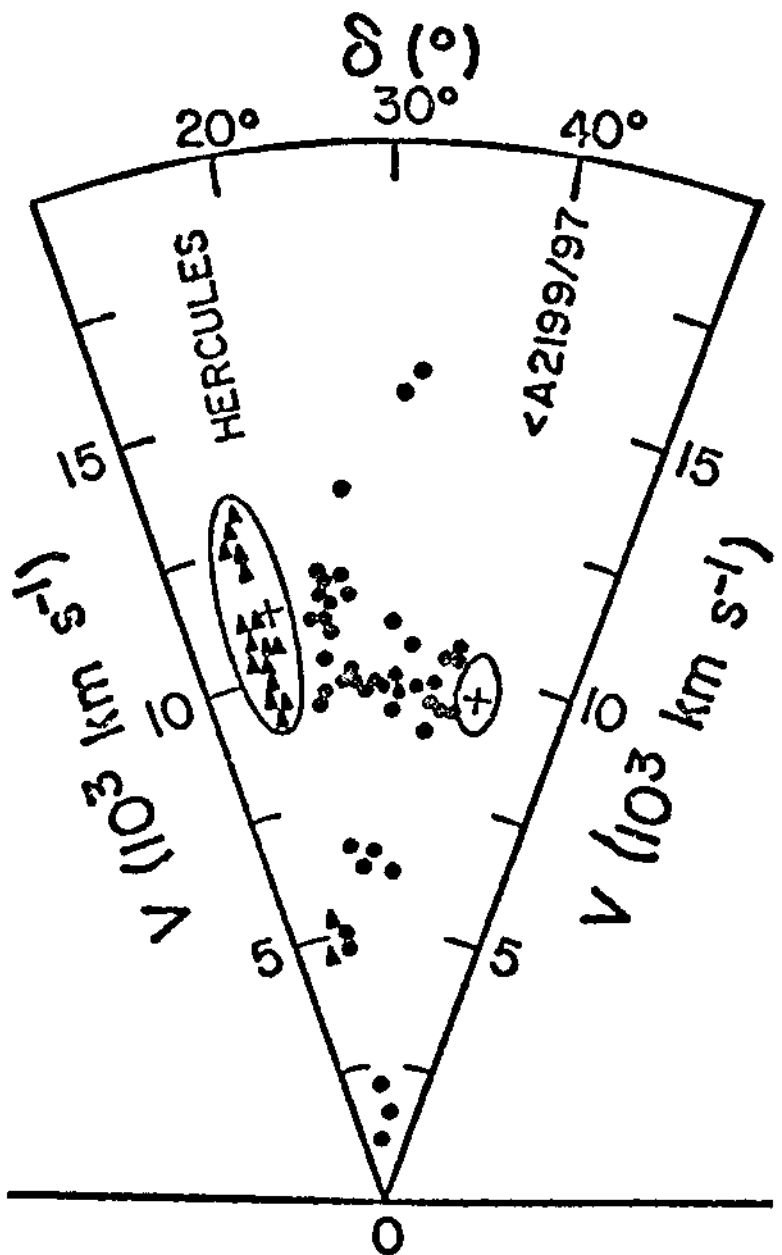


FIGURE 19 - The bridge between Hercules and A2197/A2199. This structure (with its southern extension) is the largest so far observed. The large void is also clearly visible.

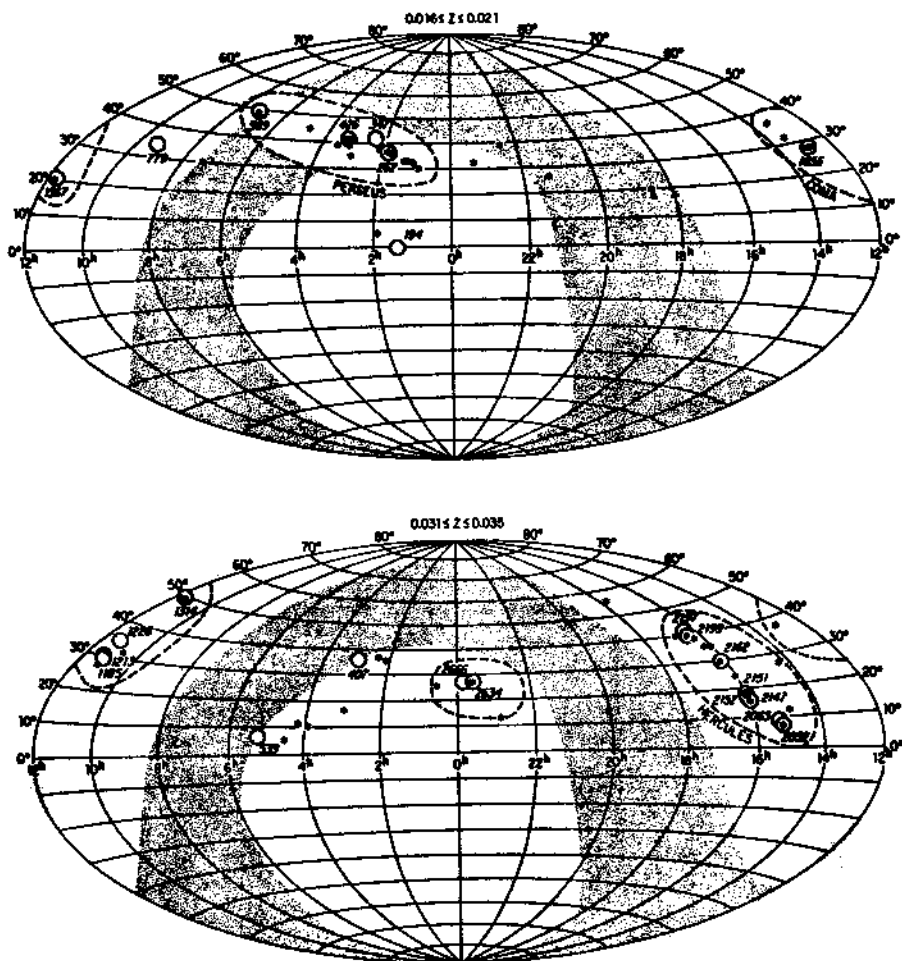


FIGURE 20 - The distribution of radio galaxies in nearby superclusters. Of particular interest is the Perseus-Pisces supercluster extending across the Galactic plane.

At the present we do not have, except for the local supercluster discussed below, detailed information on the geometry of the structures and on their kinematics. We are still limited by lack of observations at faint magnitudes. A possibility is that the superclusters are flat and extended structures as predicted by the theory of Zeldovich and collaborators (1970) and described by Einasto and his group, and/or some kind of filaments of small cross section and various shapes.

Since the Coma-A1367 and Perseus-Pisces superclusters extend in a direction almost perpendicular to the line of sight, we may be able to derive informations about their cross section and luminosity. The width of the structures as seen in their projection on the celestial sphere can be derived, for instance, by determining the HPBW on the isoplets of the region under consideration. An isoplet map for the Perseus-Pisces structure is shown in Figure 21. Here only supercluster galaxies have been mapped, $m < 14.0$.

Since the Perseus-Pisces sample is limited to rather bright galaxies, it is hard to assign cluster and group membership. For this supercluster, therefore, the results given below were computed using the whole ensemble (see also appendix). To estimate the depth of the structure in a magnitude limited sample we may proceed as follows: assuming a Gaussian number density distribution in depth

$$D(x) = (D_0/\sigma\sqrt{2\pi}) e^{-\frac{(x-x_0)^2}{2\sigma^2}} \quad (23)$$

using the Schechter Luminosity function, the redshift distribution in depth is given by the relation:

$$N(V_i, V_j) = \frac{\int_{V_i/H}^{V_j/H} x^2 D(x) \Gamma(\alpha + 1, L/L') dx}{\int_0^\infty x^2 D(x) \Gamma(\alpha + 1, L/L') dx} \quad (24)$$

where:

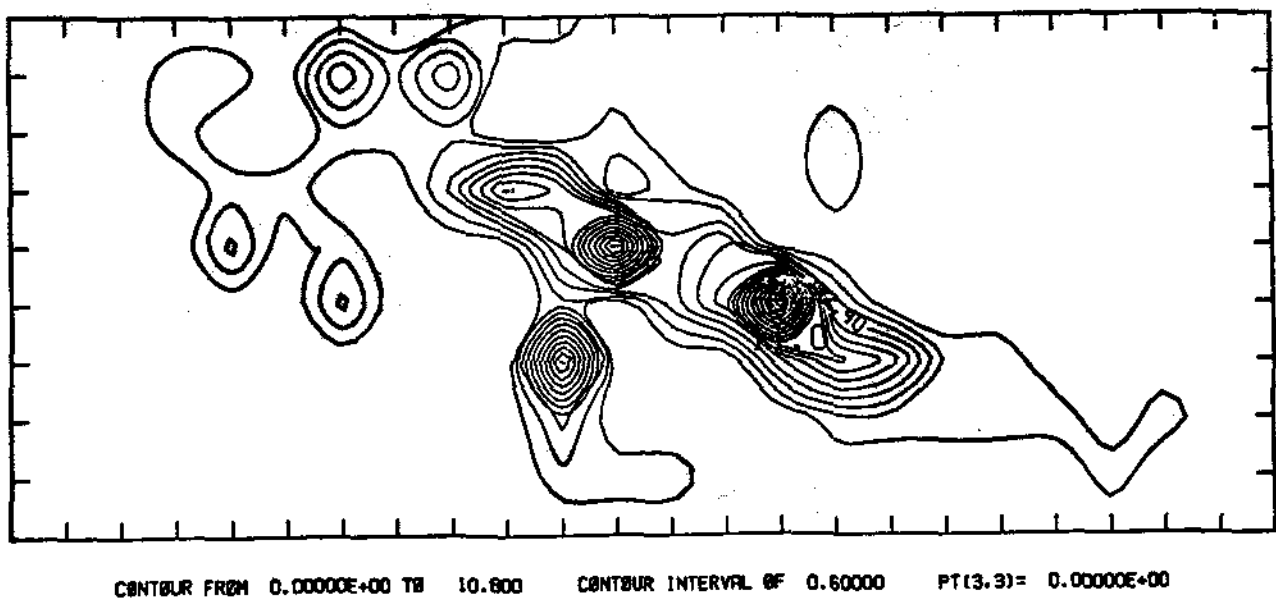


FIGURE 21 - Number density contours in the region of the Perseus-Pisces supercluster.

$x = V/H$,

Γ is the incomplete gamma function,

$$L/L' = \text{dex} [0.4(M' - m_l + 5 \log V/H - 25)]$$

and m_l = the limiting magnitude of the sample (assuming a step function for the completeness function). By minimizing the χ^2 function defined by the theoretical distribution, $N(V_i, V_j)_{\text{Theo}}$ and the observed distribution, $N(V_i, V_j)_{\text{Obs}}$ we derive the free parameters of the fitting σ and x_0 , which are respectively the depth and the distance of the supercluster structure. For the Perseus-Pisces supercluster the value of the depth determined is, however, an upper limit due to the contamination introduced by the virial velocity of the embedded groups and clusters. Note however that the procedure is somewhat uncertain when applied on small samples. The redshift cut off, at large redshifts, is due to the combined effect of distance, through the function $\Gamma(\alpha + 1, L/L')$, and assumed model, e^{-x^2} dependence. The luminosity function may, therefore, simulate a density effect. This part is at the present under investigation.

By the above procedure we estimate (Chincarini et al., 1981):

Width on the celestial sphere:

Coma/A1367 (HPW) = 700 km/sec

Perseus/Pisces (HPW) = 580 km/sec

Depth from fitting distribution in redshifts:

Coma/A1367 = 385 km/sec

Perseus/Pisces < 610 km/sec

The comparison between the observed and theoretical distribution in velocities is given in figure 22 for the dispersed component in the supercluster Coma-A.367 and in figure 23 for the ensemble of objects in the Perseus-Pisces supercluster.

The indication we have so far is therefore that such structures are rather thin. In the case of the Perseus-Pisces supercluster it seems fairly certain that also the width of the supercluster is narrow so that this supercluster may look more like a filament than a pancake.

I am inclined to believe that we are bound to find structure of various geometrical forms so that, observationally, I am hesitant in defining a shape until more observations will tell us better what we are in fact observing. The luminosity (or the luminous mass, if we multiply by a factor $\langle M/L \rangle$) can be derived either by using the above model or, in a more direct way, by multiplying the galaxian luminosity by an incompleteness factor. The details are given in appendix 4 and Chincarini et al. (1981).

We derive:

Mean Luminous Mass (assuming $M/L = 10:0$)

Coma/A1367/M = $9 \cdot 10^{13} M_\odot$

Perseus/Pisces M < $1.1 \cdot 10^{15} M_\odot$

With a supercluster volume of the order of $5 \cdot 10^3 \text{ Mpc}^3$ (the volume is of course limited to the surveyed region) we have a density of about (using $M = 10^{14} M_\odot$) $\rho = 1.5 \cdot 10^{-30} \text{ g/cm}^3$. This is an estimate for the dispersed component, the mass of the clusters of galaxies is not taken into account. The column density would be of about $\sigma = 4.5 \cdot 10^{-5} \text{ g/cm}^2$ or higher for those structures which do not extend perpendicular to the line of sight. The value is therefore a lower limit. Oort et al. (1982) interpreting the quasar absorption line as due to hydrogen in the supercluster structure derives a column density of about $7 \cdot 10^{-4} \text{ g/cm}^2$. This would indicate that the process of galaxy formation is not a very efficient one at least in regions which are outside clusters.

However, Sargent et al. (1982) find that the absorption lines in a pair of quasars whose lines of sight separation is less than 1 Mpc H^{-1} at $z = 2.5$ have no measurable cross-correlation. This would contradict the proposal by Oort et al.

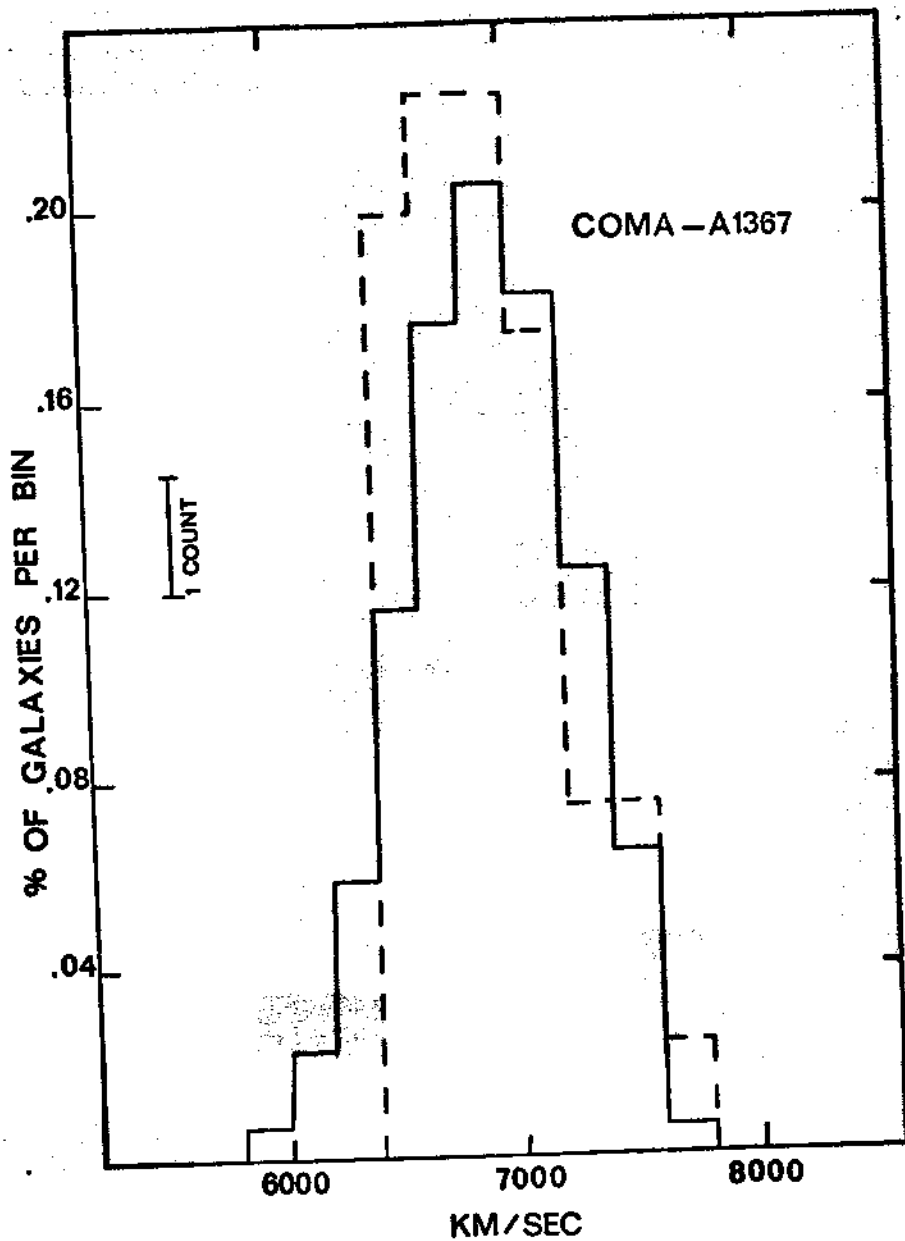


FIGURE 22 - Distribution of redshifts from the dispersed component of the Coma A1367 supercluster. Dashed line, observed distribution, continuous line, theoretical distribution according to the model described in the text.

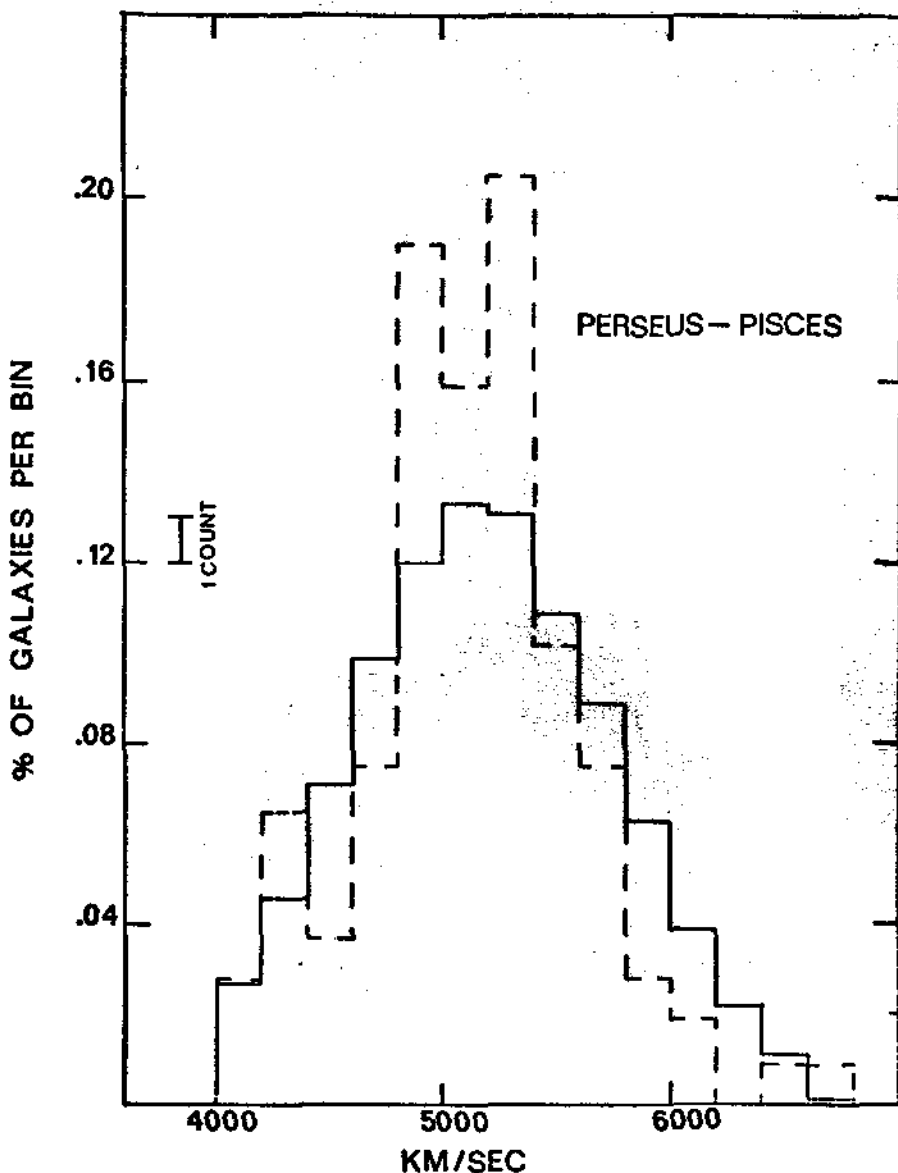


FIGURE 23 - Distribution of redshifts for galaxies, $m \leq 14.0$, in the Perseus-Pisces supercluster. Same code as in Figure 22.

The observational data I discussed are in agreement with the finding of other surveys. Kirshner et al. (1981) detected large scale structures and low density regions in randomly selected regions of the sky. Their observations add considerably to the significance of the previous findings since their samples were selected in a completely different way. Particularly important is the survey carried out by Davis et al. (1980). These authors observed about 2400 galaxies brighter than $m = 14.5$ reaching, therefore, regions beyond the local supercluster. Thanks to the use of one of the recently developed digital detectors, they also reach an accuracy of about 40 km/sec in the determination of the redshifts. The authors confirm that the space distribution of galaxies is frothy, characterized by large filamentary superclusters of up to 60 Mpc in extent, and corresponding large regions void of galaxies, figure 24.

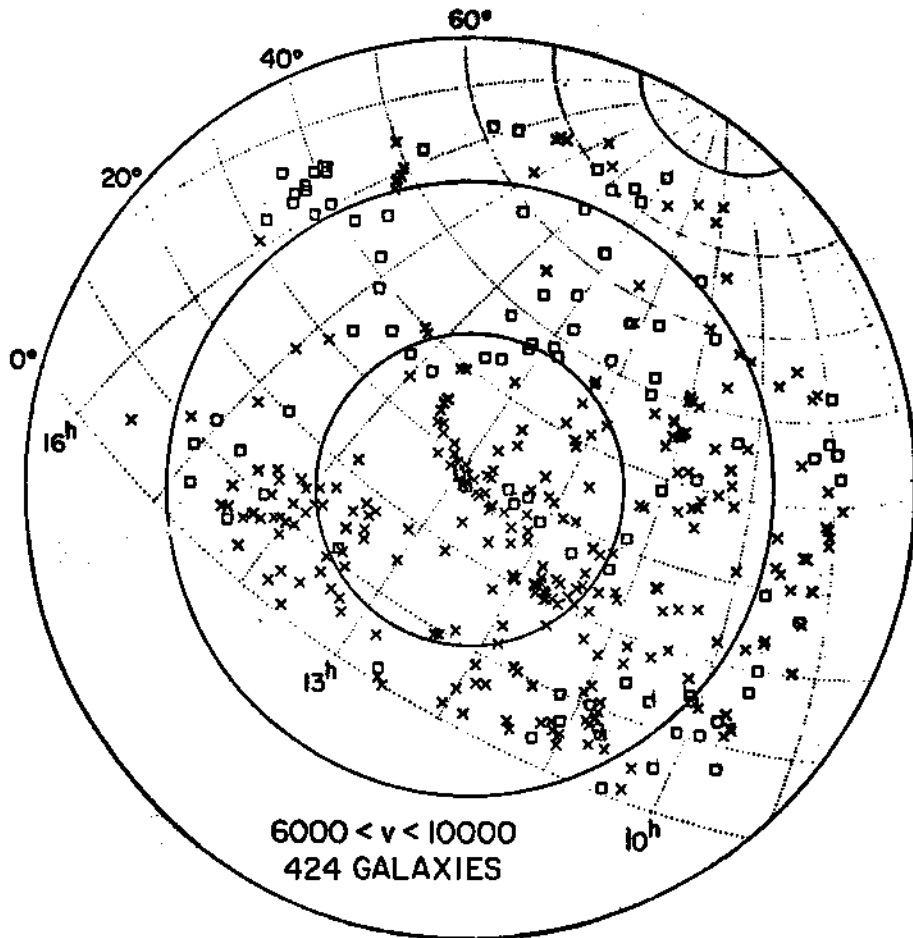


FIGURE 24 - Distribution of galaxies in the redshift range 6000-10000 km/sec according to Davis et al. (1981). Crosses refer to redshifts between 6000 and 8000 km/sec. Squares refer to redshifts between 8000 and 10000 km/sec.

Now that we have formed an idea on the space distribution of galaxies it is interesting to go back to the two dimension distribution and see if some of these structures can be recognized and may in fact extend beyond the limits of the regions surveyed for redshifts. The maps I will show have been made using data from the Zwicky catalogue, most of these structures are however also visible in the maps made by Shane and Wirtanen. The region of the Coma/A1367 is reproduced in figure 25 ($m_z < 15.0$). A NE extension of the supercluster is clearly visible.

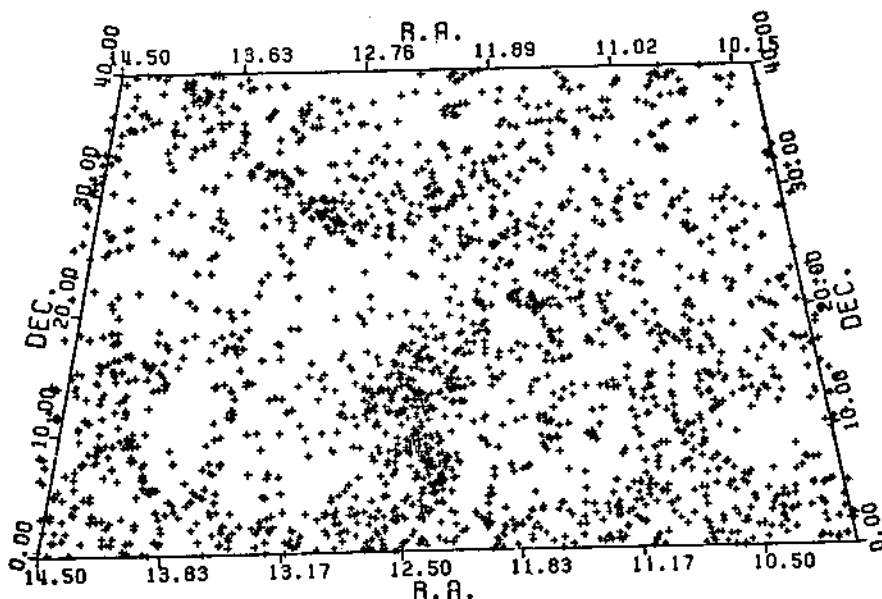


FIGURE 25 - The region of the Coma-Al367 supercluster. Virgo galaxies in the foreground $m_z < 15.0$.

The structure is somewhat better visible at fainter magnitudes, $m_z < 15.7$, and practically undetectable at $m_z < 13.5$, figure 26. As can be seen in figure 27, the Hercules supercluster

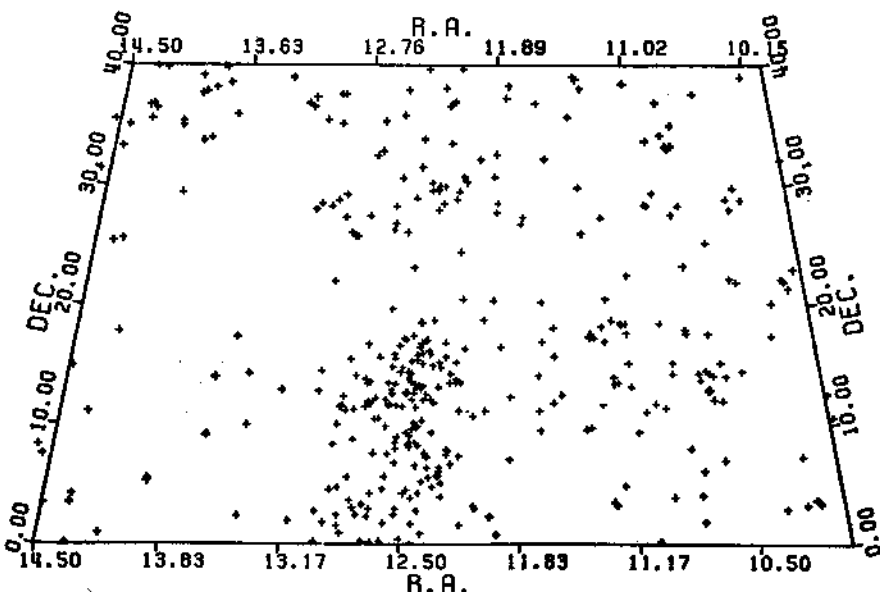


FIGURE 26 - Same region shown in Figure 25 for $m_z < 13.5$. Only the Virgo structure is clearly visible.

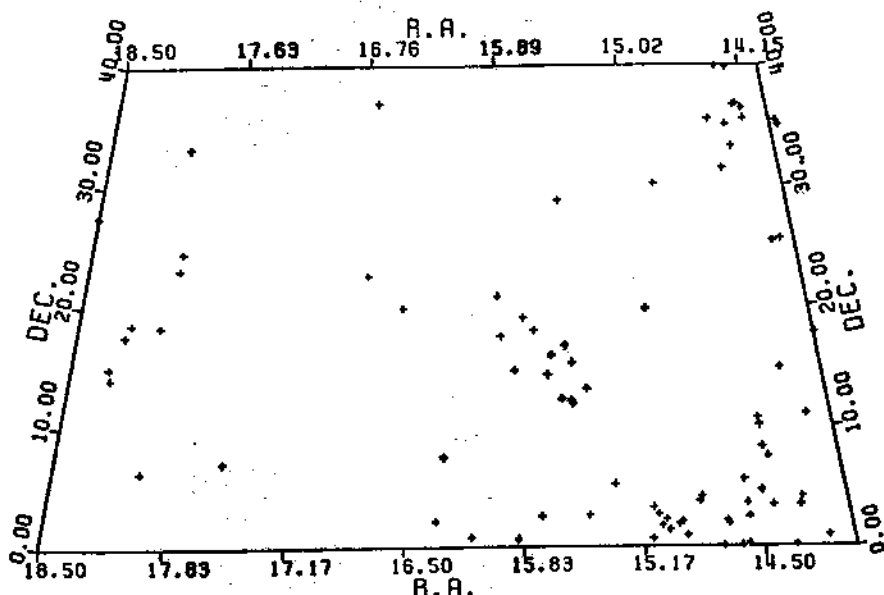


FIGURE 27 - Region of the Hercules supercluster. No structure is discernible at $m_2 \leq 13.5$.

if completely undetectable at $m_2 < 13.5$, however at fainter magnitudes, $m < 15.5$, the eye detects a certain continuity from the clusters A2197/99 toward the Hercules region and south west toward the region of the Serpens - Virgo cloud, figure 28. Another structure, which is visible in the maps by Shane and Wirtanen and also evidenced by Giovanelli using published redshifts, is illustrated in figure 29. In other regions, however, where superclustering has been studied, the two dimension distribution does not give any clue. In figure 30, for instance, is reproduced the region of the sky in which Kirshner et al. (1979) selected their sample. Except for the Coma/A1367 extension, no further structure is visible in the two dimension distribution. Naturally the empty regions in the redshift space go completely undetected.

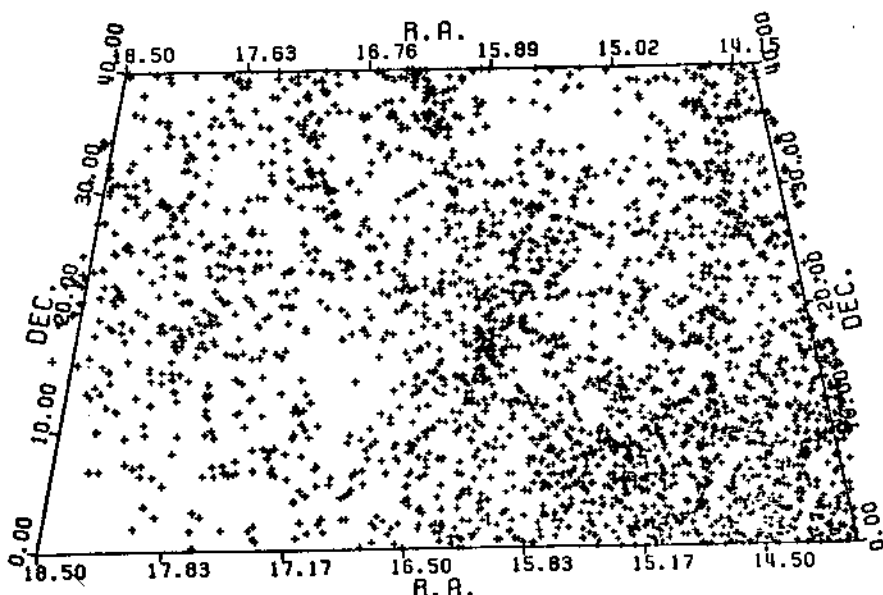


FIGURE 28 - The Hercules supercluster with its north extension toward A2197/A2199 and the southern extension toward the Serpens - Virgo cloud.

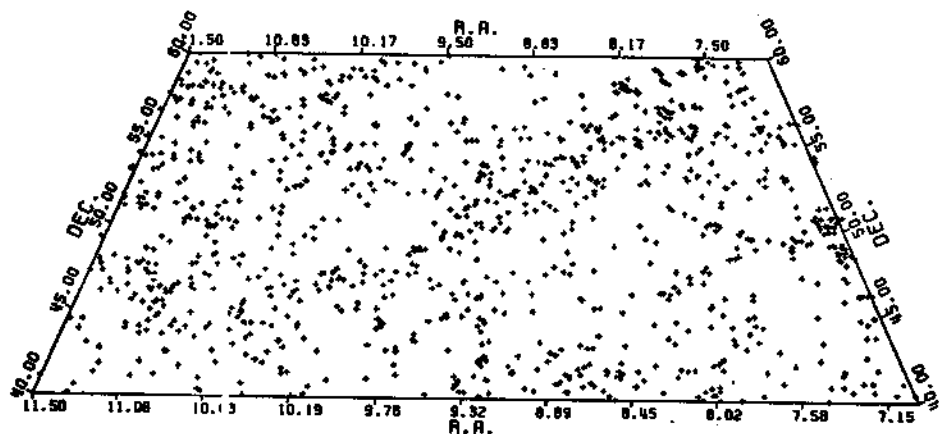


FIGURE 29 - A supercluster structure in the Ursa Major region.

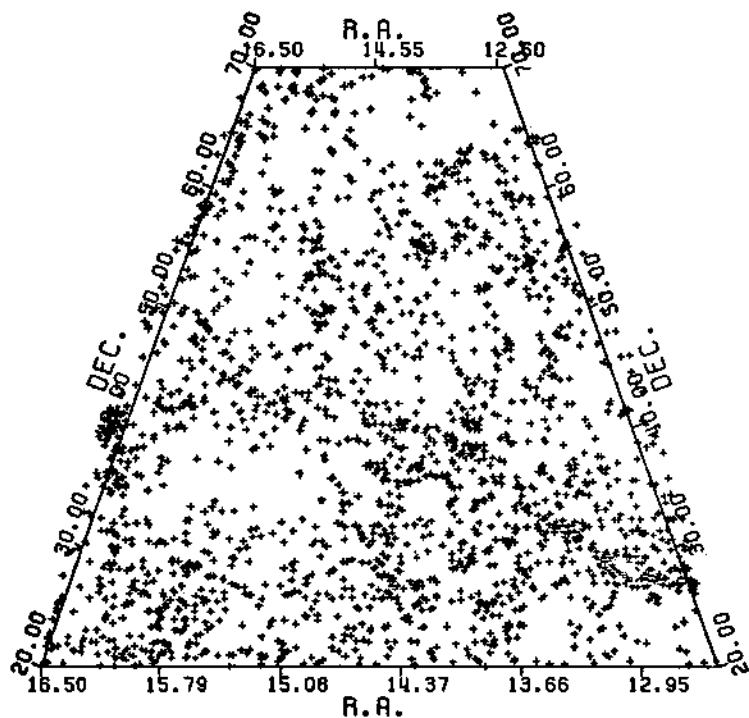


FIGURE 30 - The region of the Kirshner et al. sample. Their fields, 1.4 square degrees, were centered at: R.A. = $13^{\text{h}} 37.2^{\text{m}}$, D. = $+26^{\circ} 55'$; R.A. = $16^{\text{h}} 03.5^{\text{m}}$, D. = $+41^{\circ} 11'$; R.A. = $14^{\text{h}} 00.9^{\text{m}}$, D. = $+69^{\circ} 45'$.

Abell used clusters of galaxies as supercluster tracers, figure 31. A similar approach has been used by Corwin (1980) and by Schuch (1981). In these two fields clusters of various distance classes are concentrated in part of the surveyed region, figure 32. Nothing is visible from the distribution of Zwicky galaxies, figure 33. The question can be finally asked whether the low density regions or voids and/or positive density fluctuations could be detected using counts of galaxies and plotting $N(< m)$ versus m . The fluctuations would cause bumps in such curves which can eventually be fitted by the theoretical distribution. However the small amplitude of the bumps and the characteristics of the sample used (size of the solid angle for instance) would make such fluctuations difficult to detect and interpret.

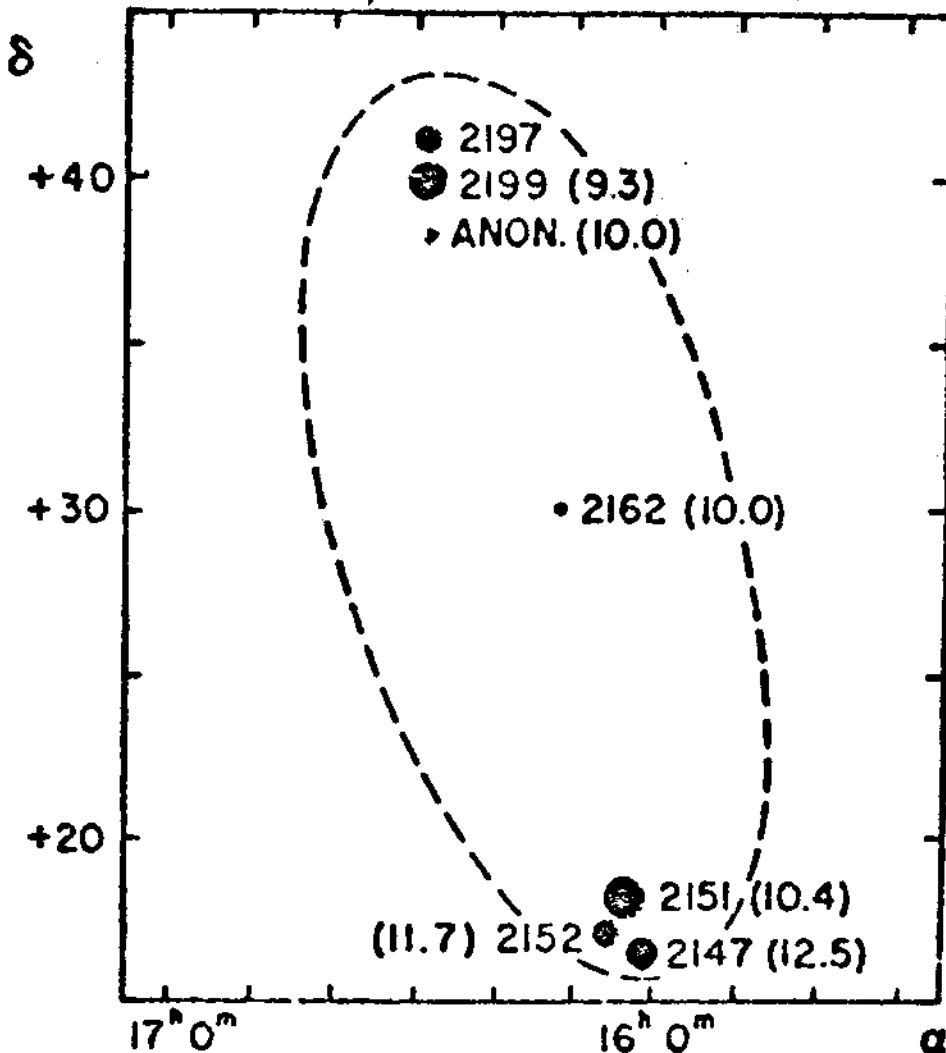


FIGURE 31 - The Hercules supercluster as identified by Abell using the distribution of clusters of galaxies.

IV - PECULIAR VELOCITIES

If in a region of space we have a mass excess δm (excess over $\langle \delta m_b \rangle = \text{volume} \cdot \langle \rho_b \rangle$ where $\langle \rho_b \rangle$ is the mean mass density of the Universe), we would observe in objects at a distance R a peculiar velocity (perturbation)

$$\delta v_p = \frac{G \delta m}{R^2} H^{-1} \quad (25)$$

The various quantities are treated in the usual way with the difference we are working with the perturbing mass or excess density rather than the background distribution of mass of the world models. The above velocity, acceleration x time, is directly related to quantities of interest:

$$\delta v_p = G R \delta \rho H^{-1} \approx G \langle \rho_b \rangle \frac{\delta \rho}{\langle \rho_b \rangle} R H^{-1} = \Omega H R \frac{\delta \rho}{\langle \rho_b \rangle} = V_H \Omega \frac{\delta \rho}{\langle \rho_b \rangle} \quad (26)$$

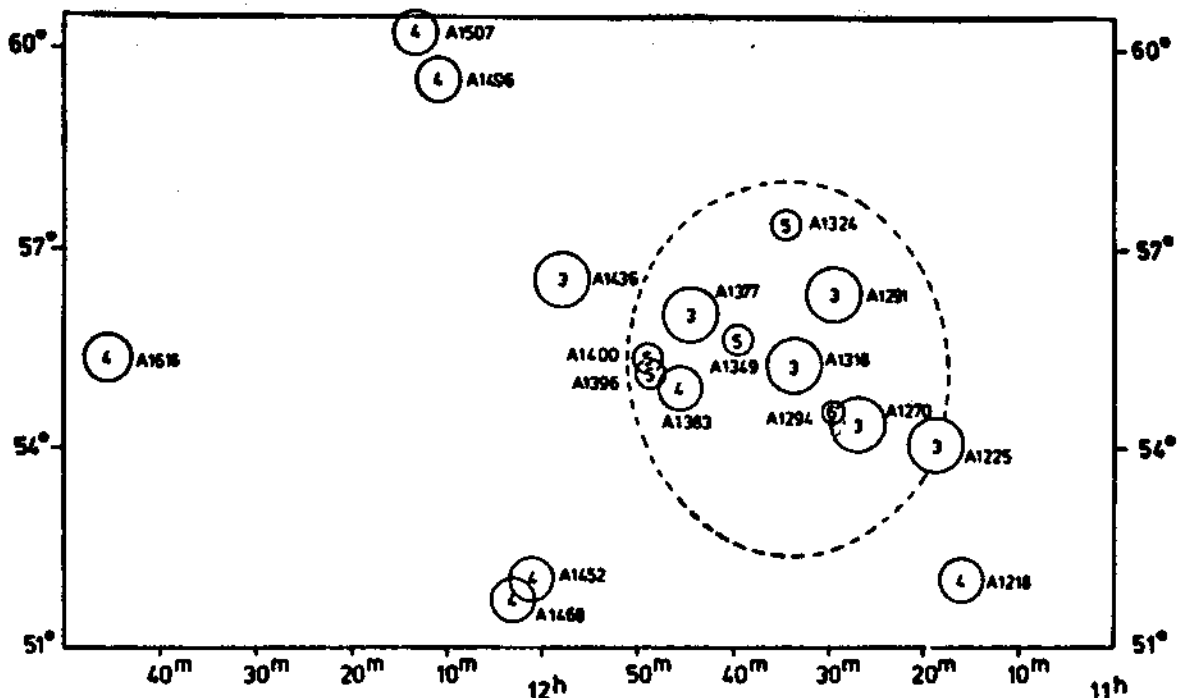


FIGURE 32 - The supercluster in the Ursus Major region identified by Schuch. Distant clusters are found in the same region or closer clusters.

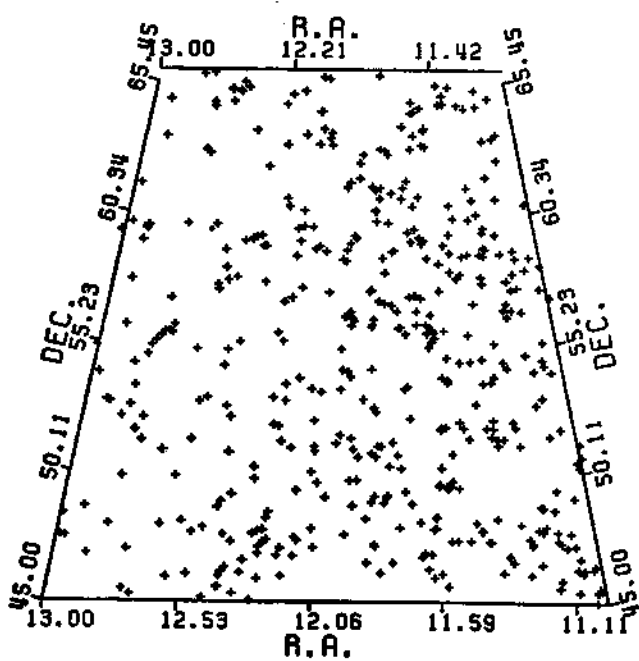


FIGURE 33 - The distribution of galaxies, $m_z \leq 15.5$ in the region of the sky studied by Schuch. No structure is visible in the two dimension distribution.

where

$$\Omega = \langle \rho_b \rangle / \rho_c = 8/3\pi G \langle \rho_b \rangle / H^2 \quad (27)$$

and

$$\delta\rho = \rho - \langle \rho_b \rangle \quad (28)$$

which shows that measurements of peculiar velocities (streaming motion) and density fluctuations are a measure of the mean mass density of the universe. This method of measurements is particularly useful when applied to the local supercluster where there is a large fluctuation in the region of Virgo. Since the observed voids are extended and represent high negative density fluctuations, they also influence the kinematics of galaxies.

In a more general context we ask the question of motion of galaxies and the capability to separate the various components, that is Hubble velocities, virial velocities, streaming velocities, relative motion of clusters and superclusters, peculiar velocities of galaxies. Such determinations are affected by membership assignment and selection effects (magnitude limited samples) in the studies of individual groups and by the difficulty of evaluating the results in a statistical approach. As a consequence our knowledge on the velocity field is still limited. Estimates on peculiar velocities (non-Hubble motion) range from values less than 50 km/sec (Braduardi et al., 1981) to a few hundred km/sec. Such differences however, seem to reflect the simple fact that the various samples are measuring different things, isolated galaxies and groups.

The statistical method used by Geller and Peebles (1973) to measure velocities outside great clusters may have interesting applications in the study of the large scale structures. In a three dimensional map, where the redshift is taken as a measure of distance, a non-Hubble velocity component transforms a spherical system into a structure elongated along the line of sight, an effect which is clearly visible in clusters of galaxies. A measure of such distortion is a measure of the peculiar, non-Hubble, velocity. If II and σ are the components of the separation parallel and perpendicular to the line of sight, the probability for a galaxy to be found in the volume element $\delta\pi\delta A$ at distance (II, σ) from a randomly chosen galaxy is:

$$\delta P = \langle n \rangle \left[1 + \xi(\sigma, II) \right] \delta II \delta A \quad (29)$$

In an anisotropic distribution the autocorrelation function depends on both the separations σ and II. The effect of peculiar velocities is to elongate the autocorrelation function in the σ direction compared to its distribution in the II direction. In other words the additional effect of a peculiar velocity increases the separation between objects in the redshift dimension. The analysis, applied on some of the existing data, gives a velocity dispersion of about 400 km/sec. It can be shown that such a value is a measure of the mean density. Peebles et al. (1980) derived $\Omega = 0.8$, a rather high value. Observational errors may slightly affect such determinations, so that new samples may give a better measure of these quantities.

The velocity dispersion of isolated galaxies of clusters of galaxies (deviation of the first ranked galaxy from the magnitude-velocity correlation line) is rather low. Tamman et al (1980). One of the best places of evidence supporting this is the fact that large peculiar velocities would produce more negative redshifts in the non-cluster region of Virgo.

Peculiar velocities could originate as virial motion in a bound supercluster or reflect the velocity of a rotating structure. Both these possibilities have been discussed in the literature. I believe such models are unlikely. In the Hercules supercluster, if the redshift of the embedded clusters is interpreted as a radial virial velocity we obtain a mass which is of an acceptable order of magnitude. It is not clear. However, how to virialize such structures within a Hubble time.

Rotation is hard to detect and difficult to interpret. Even assuming it is detectable and the velocity field can be unambiguously interpreted as rotation (to do this we need a measure of the distance which is independent of redshift) it could be due to primordial vorticity. A

particle at a distance of 20 Mpc from the center of rotation has a period $P = 10 \cdot H_0^{-1}$ assuming a supercluster mass $m_{sc} = 10^{15} m_\odot$.

Are superclusters moving relative to each other? We have no evidence one way or the other. The present data are not enough and not accurate enough to answer the question. Disturbing observations exist however. Rubin et al. (1976) find that the average line of sight velocities of a sample of Sc galaxies distributed in a shell which is approximately at a distance of 90 Mpc is a function of the direction in which we look. The anisotropy in the measure of H_0 is interpreted (due to its sine dependence on the supergalactic longitude) as due to a component of motion of the local group in the direction of the Perseus-Pisces supercluster (after applying corrections for the rotation of the galaxy and for the component of motion of our galaxy toward Andromeda). The result is supported by the findings of Visvanathan who analyzed a sample of E, SO galaxies. Such anisotropy may be related to the motion of superclusters relative to the local supercluster, or be spurious and due to uncertainties and biases caused by the inhomogeneous distribution of galaxies in the universe.

V - AN INTERESTING CORRELATION

As I mentioned above, past attempts to measure rotation of clusters of galaxies have been inconclusive. Similarly inconclusive were the various attempts to evidence

- 1 - a non-random distribution in the position angle of the major axis of member galaxies or
- 2 - a correlation between the position angle of galaxies and the P.A. of the cluster major axis.

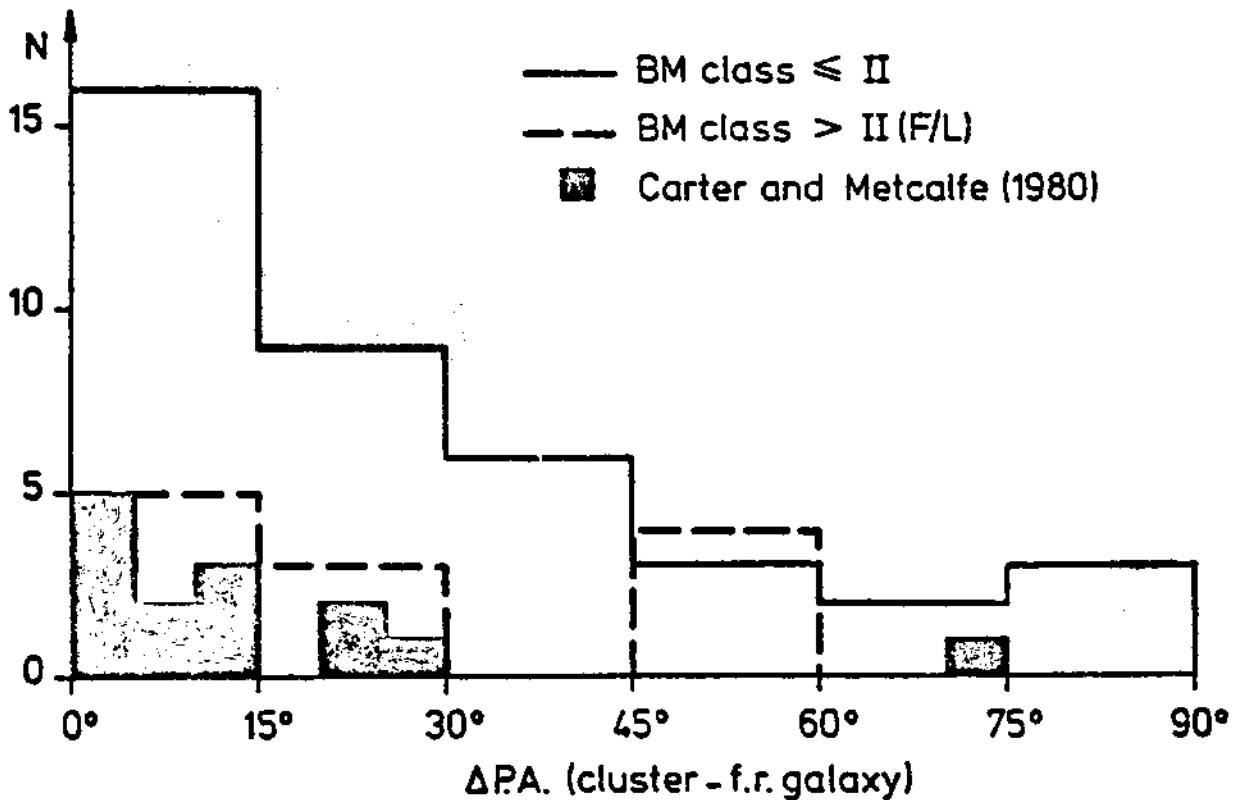


FIGURE 34 - Distribution of the difference between the position angle of the first ranked cluster galaxy and the position angle of the cluster major axis (Binggeli, 1981).

More recent observations, however, both in the x-ray, Braduardi et al. (1981) and in the visual Mac Gillivray et al. (1976), Schipper and King (1978), Carter and Metcalfe (1980) have shown that clusters of galaxies are not symmetric. According to Carter and Metcalfe, the distribution of apparent ellipticities peaks at about $e = 0.45$. Even more remarkable is the effect detected by the authors of the alignment between the position angle of the CD galaxy and the cluster semi-major axis (1). Such distribution and correlation has been confirmed by Binggeli (1981), figure 34, who went a step further. He finds that neighbor clusters tend to point to each other. He gives also some evidence that neighboring clusters, within a distance of 100 Mpc, are preferably found along the axis defined by the orientation of a cluster (or its first ranked galaxy). Similar features are apparent in the contour map of the Perseus-Pisces supercluster, figure 21. The main condensations tend to be aligned toward each other and, at larger distances from the density peak, they tend to follow the main distribution of the supercluster. The position angle of the major axis of the x-ray extended emission in the Perseus (A426) cluster is P.A. = $92^\circ \pm 5^\circ$, and the cluster center determined from galaxy counts lies 6.4 Southwest of the x-ray centroid, Braduardi et al. (1981). These results fit very well with the large scale distribution of matter described above, give further evidence that we are interpreting the observations correctly, and point to tidal effects which occurred during the formation processes.

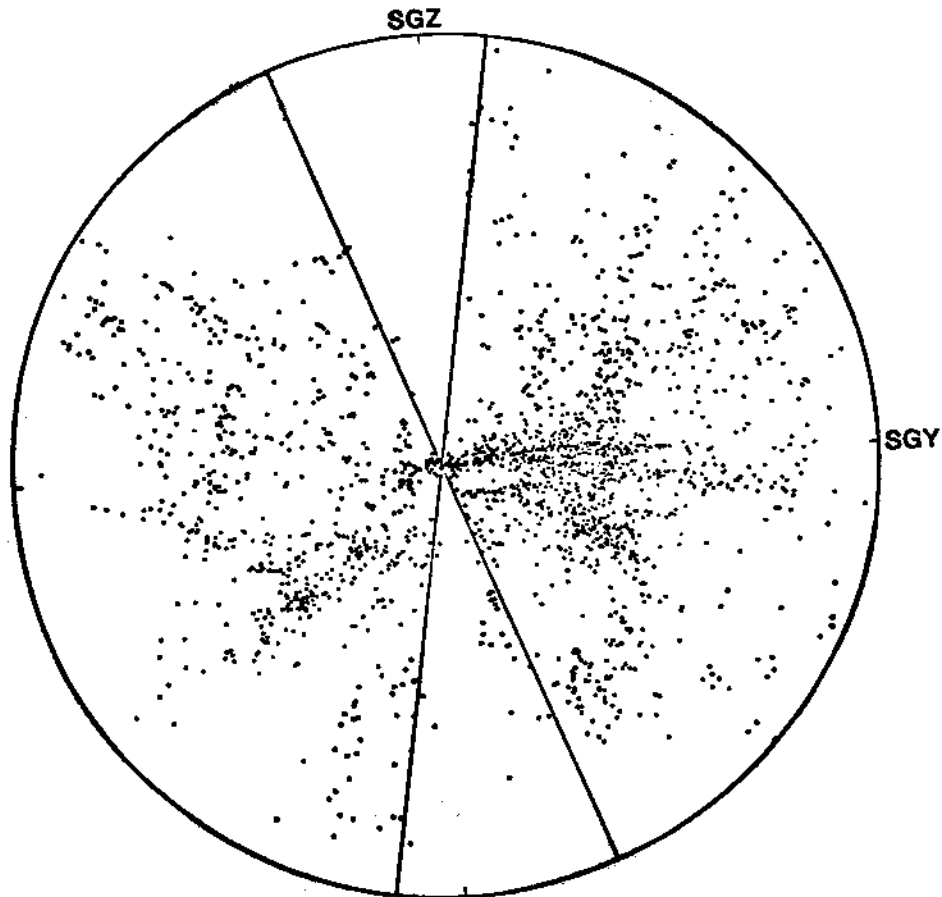


FIGURE 35 - Galaxies in the Fisher and Tully catalog projected into the SGY-SGZ plane. The system of coordinates is defined so that the SGZ axis points in the direction SGB = $+90^\circ$, the SGX axis is aligned toward SGL = 0 and the SGY axis points in the direction SGL = 90° , SGB = 0° . The SGX, SGY plane define, therefore, the supergalactic equator, while the SGX, SGZ plane almost coincides with the plane of the galaxy. The outer boundary, has a radius of $30 h^{-1}$ Mpc. (From Tully, 1981).

(1) The correlation was first evidenced by G.N.Sastry, 1968, P.A.S.P., 80, 252.

VI - THE LOCAL SUPERCLUSTER

As I have said, the local supercluster has been recognized since the work of Shapley and Ames and studied in detail by various astronomers, in particular by de Vaucouleurs (1953). Due to the fact that we are part of it and not too far from the Virgo cluster studies on the subject developed, to some extent, independently, earlier and differently from the work in other regions of space. The literature, therefore, may sometimes give the impression that we have on one hand the local supercluster and on the other hand the rest of the universe. The local supercluster is not a single or peculiar structure or has any peculiarity except for the fact that we are part of it. The vicinity of the galaxies allow detailed studies which may give us clues in understanding the large scale structure of the universe. Vice versa a better knowledge of the large scale structure may help us in better comprehending the local phenomena.

An extensive study of the distribution of galaxies up to a distance of about 51 Mpc ($h=100 = 0.5$) has been recently published by Tully (1981).

As can be seen from figures 35 and 36 the distribution of galaxies defines a pseudo plane(the supergalactic plane) on which the main concentration, the Virgo cluster, is clearly visible near the central region. (The center is defined by the Virgo cluster which is where we find the maximum density of galaxies, the center so defined may be completely unrelated to a geometrical center which could be, somehow, defined). The distribution of redshifts, Virgo

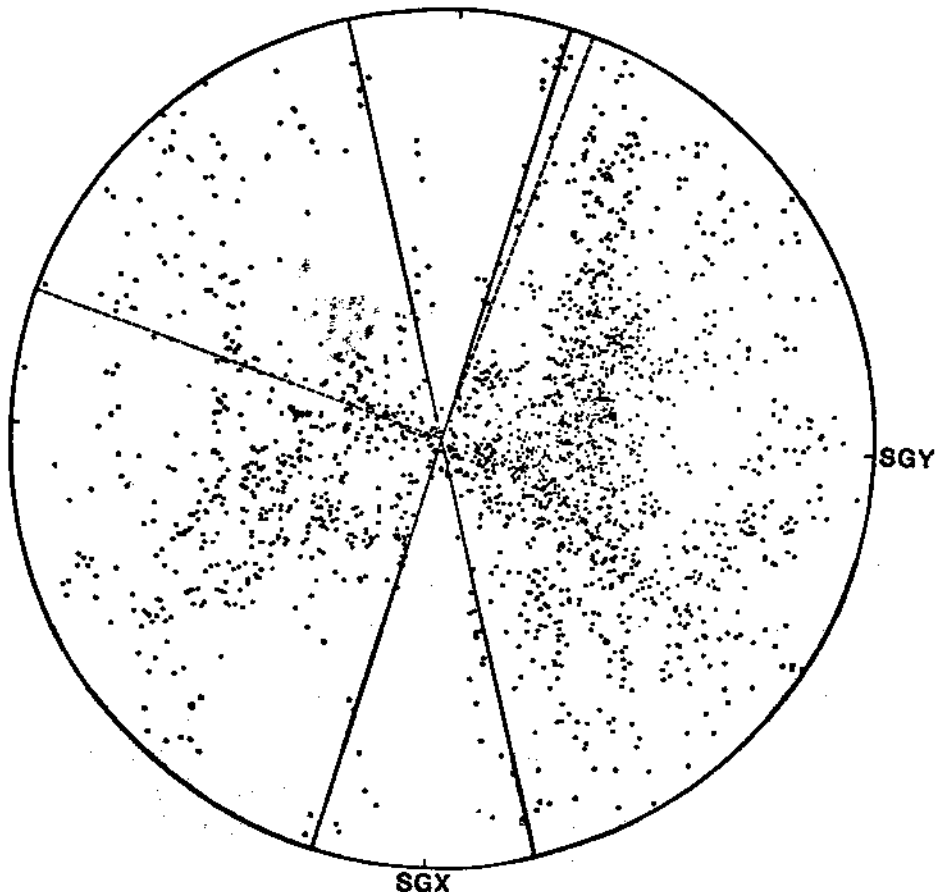


FIGURE 36 - Same galaxies of figure 35 projected into the SGX, SCY plane with marked the zone of avoidance and the zone of incompleteness. The concentration due to the Virgo cluster is clearly visible. Also note that figure 35 gives the impression of a structure seen edge-on while in figure 36 the structure is seen about face on. (Tully, 1981).

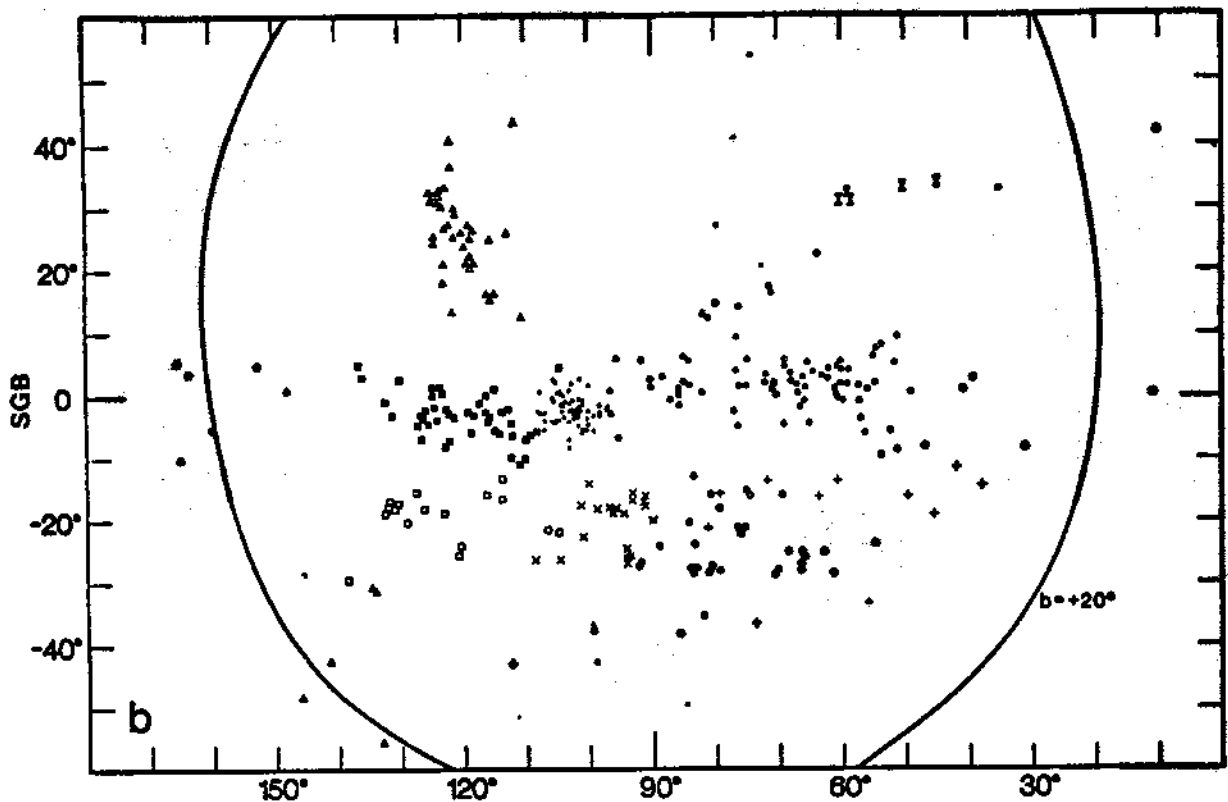


FIGURE 37.A - The figure refers to a complete sample of galaxies brighter than $M_B = -19 + 5 \log h$ and contained in the volume: $|SGX| < 10 h^{-1} \text{ Mpc}$, $SGY < 15 h^{-1} \text{ Mpc}$ and $|SGZ| < 10 h^{-1} \text{ Mpc}$. It is clearly seen that (1) most of the galaxies belong to well identified groups and (2) most of the supercluster is void of visible matter. The symbol code is as follows: Canes Venatici (*), Virgo II (), Virgo III (Δ), Leo (o), Crater (), Leo I (x), Leo Mi (+), Antlia (Δ), Draco (x), NGC5643 (*) and unassigned (-). (Courtesy of B.Tully).

cluster excluded, is interpreted by Tully as due to two components. One associated with the flattened disk of the local supercluster and the other (containing 40 percent of the bright galaxies) associated with a *halo*. The more detailed distribution shows that the vast majority of galaxies reside in a small number of discrete structures so that most of the volume is in fact quite empty, see for example figure 37 a,b. Tully, Figure 38, also calls attention to the fact that some of the clouds are elongated in the direction of the Virgo cluster. If this is due to a tidal action at an earlier epoch, see for instance Binney and Silk (1979), then it may be possible to estimate the epoch of formation. The reasoning used by the author is as follows: let us consider a perturbing object with a density distribution and at a distance R a perturbed object. Using the Roche criterion, the tidal radius is

$$R_T \propto (m/\delta m)^{1/3} R \quad (30)$$

where m is the mass of the perturbed object and δm the excess mass (density enhancement) causing the tide. Since δm expands in the Hubble flow:

$$\delta m/R^3 = \frac{m - m_B}{R^3} \propto \rho - \langle \rho_b \rangle = \frac{\delta \rho}{\langle \rho_b \rangle} \langle \rho_b \rangle \propto t^{2/3} t^{-2} = t^{4/3} \quad (31)$$

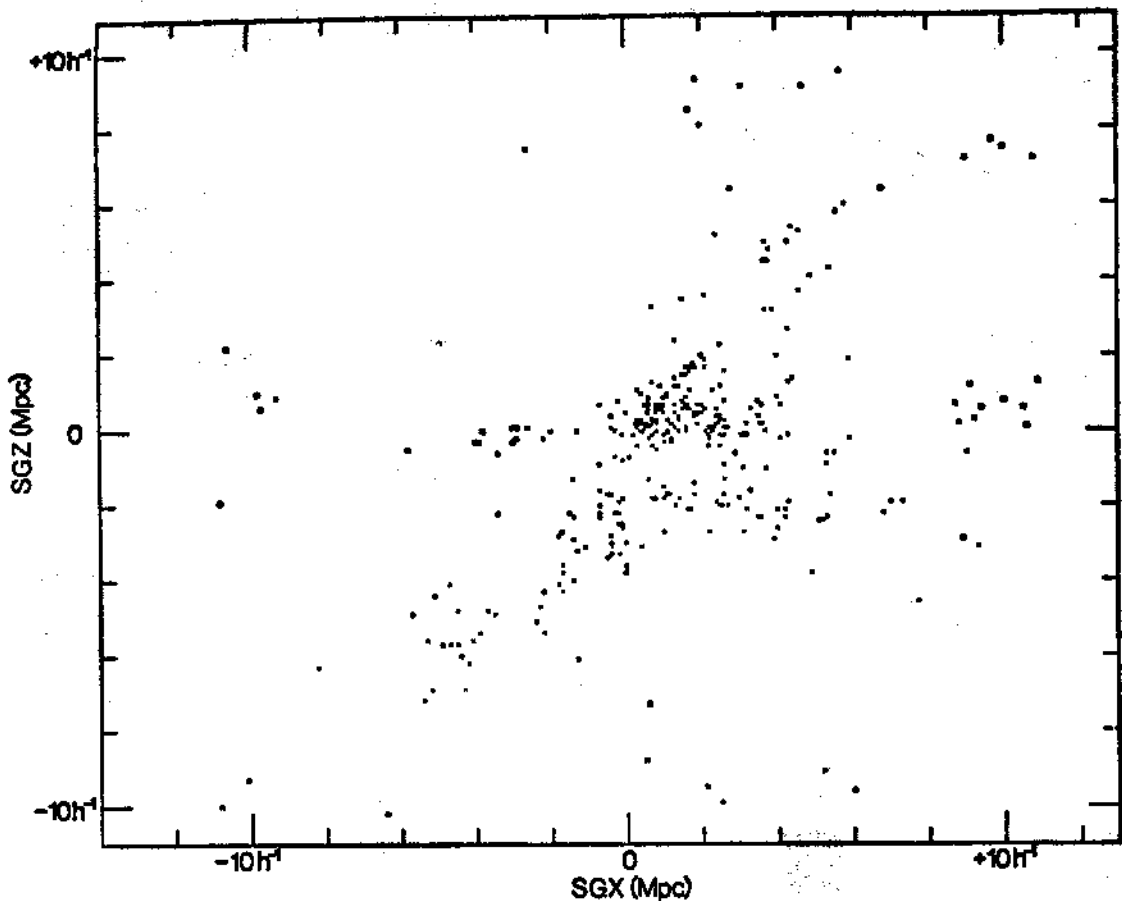


FIGURE 37.B - The empty zone is quite evident in projection into the SGX, SGZ plane. (courtesy from B.Tully).

where m_B background mass = $4/3\pi R^3 \langle \rho_b \rangle$ with $\langle \rho_b \rangle$ mean mass density using

$$1+z \approx (t_0/t)^{2/3}; \quad \delta m \approx \delta m_0 (R/R_0)^3 (1+z)^2 \quad (32)$$

or

$$1+z \approx (m/\delta m_0 (R_0/R_T)^3)^{1/2} \quad (33)$$

where the subscript refers to quantities measured at the present epoch. The quantities on the right side of the equation can be estimated since: R_0 is the distance of the perturbed object from the Virgo cluster, R_T about twice the present RMS radius, a measure of the size at maximum expansion during the process of virialization, and

$$m/\delta m_0 \approx N(\text{group})/(N(\text{within } R)) - \langle N \rangle \quad (34)$$

where $\langle N \rangle$ is the mean number of galaxies in the universe. Tully derives $z = 8$. This estimate is in agreement with theoretical determinations of the time of formation. Miller's numerical models, for instance, show that such structures begin to be discernible from the background at a redshift of about $z = 15$.

The first clear evidence that the local group has a non-Hubble velocity component came from

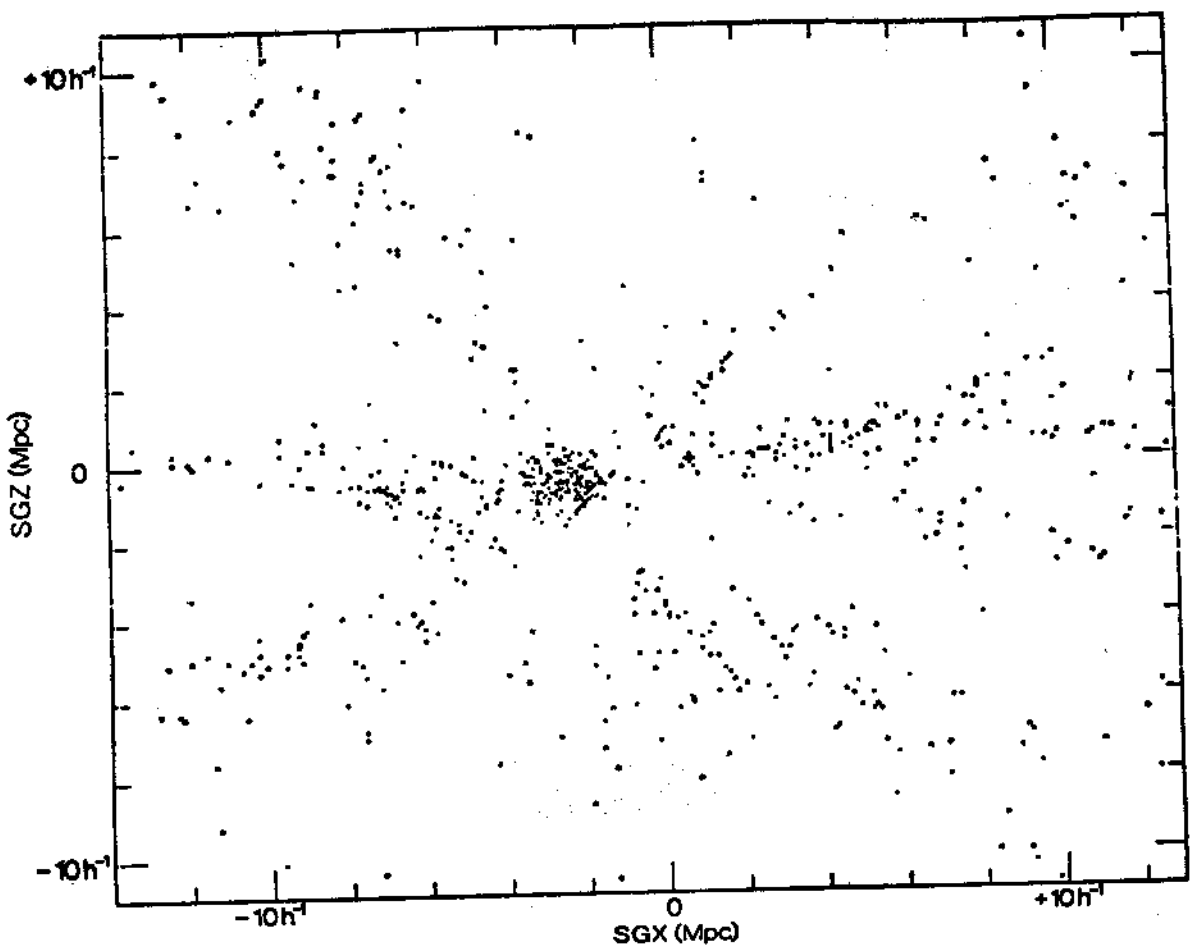


FIGURE 38 - The radial elongation of the clouds, pointing to Virgo.

the observations of a dipole anisotropy in the temperature of the microwave background. If we are immersed in a sea of blackbody radiation at temperature T_0 and moving at speed V relative to the frame of the radiation, then

$$T(\theta) = T_0 (1 - V^2/C^2)^{1/2} (1 - V/C \cos \theta)^{-1} \quad (35)$$

$$= T_0 (1 + V/C \cos \theta) + \frac{\Delta T}{T} = V/C \cos \theta \quad (36)$$

for $V/C \ll 1$ where θ is the angle between the direction of motion and the direction we measure the temperature. The anisotropy retains a Planck spectrum.

The observations give $T = 3$ m K in the direction R.A $11^h 36^m$ and D. $-2^\circ 1 = 269^\circ 13'$, $b = 55^\circ 45'$. (See Review article by Weiss). Interpreting it as due to the motion of the local group:

$$V(2.7 \text{ K}) \approx 340 \text{ km/sec} \quad (37)$$

After correction for galactic rotation (250 km/sec) and a component of motion of our galaxy toward M31 (80 km/sec) the motion of the local group is about 570 km/sec in the direction R.A. $\approx 11^h$ and D. $\approx -24^\circ 1 = 273^\circ 21'$, $b = 32^\circ 16'$.

Yahil et al. 1980) find that the streaming velocity of galaxies is in the general direction of the microwave background anisotropy, the intensity of the velocity vector is, however, only

245 ± 50 km/sec. The difference is more significant in the direction of the Virgo cluster. Other determinations Davis et al. (1981) suggest an infall velocity of about $300 - 500$ km/sec in the general direction of Virgo (the coordinates of the Virgo cluster are: R.A. = $12^{\text{h}} 27^{\text{m}}.6$, D. = $12^{\circ} 56'$; I = $282^{\circ} 52'$, b = $74^{\circ} 41'$). See also Aaranson et al. (1980). The most recent analysis, Schechter et al. (1980), give a total velocity toward the Virgo cluster of 331 ± 41 km s $^{-1}$ with a possible rotational component about the center of the Supercluster of $180 \pm$ km s $^{-1}$ at the position of the local group. A value of 400 km/sec seems to be a good approximation. Lower values, with however larger errors, have been estimated by Schechter (1980) using a sample of elliptical galaxies - Virgocentric flow about 190 ± 130 km/sec and by Sandage and Tamman using supernovae, infall velocity about 162 ± 180 km/sec. As mentioned in section VI the streaming velocity is interpreted as due to an excess of mass at the location of the Virgo cluster. With an estimated excess of about $\delta\rho/\rho = 2.0$ we have $\Omega \approx 0.4$. Using the derivation by Clutton Brock and Peebles (1981) based on the mass clustering implied by the autocorrelation function

$$\delta v_p/V_H \approx \delta N/N \cdot \Omega \approx 4.24 \cdot 10^4 V_H^{-3/2} \Omega \approx 1.34 \Omega \quad (38)$$

where I used $V_H = 1000$ for Virgo. A streaming velocity of about 400 km/sec implies therefore a value of $\Omega \approx 0.3$. The perturbation in the velocity field caused by a mass excess in the Virgo region is depicted in figures 39 and 40. Note that in some direction the redshift is not univocally related to distance. When a larger volume of space is considered, $70 < d < 130$ Mpc, the solar system moves in the direction R.A. = 2^{h} and D = 53° with a velocity of 600 ± 125 km/sec. This corresponds to a motion of the local group in the direction R.A. = $4^{\text{h}} 30^{\text{m}}$ and D = 40° (I = $165^{\circ} 57'$, b = $-11^{\circ} 32'$) at a speed of about 395 km/sec, Rubin-Ford effect (Rubin et al., 1976). The direction coincides approximately with the position of the Perseus-Pisces supercluster.

The situation is somewhat confused by two main factors:

1 - The Rubin-Ford effect is detected also in samples with $V \approx 2500$ km/sec, Visvanathan that is it may involve smaller scale motion and either be at variance with the infall velocity or reflect motions within the supercluster;

2 - The uncertainties are still very large, solution 5 of Schechter (1977), for instance, differs by about 50° in longitude from the solution given by Rubin et al. As an example of the components of motion we find, using $V_{\Theta} - V_{MW} = 380$ km/sec in the direction R.A. = $11^{\text{h}} 36^{\text{m}}$ and D. = -2° and $V_{\Theta} - V_{LG} = 336$ in the direction R.A. = $23^{\text{h}} 20^{\text{m}}$, D. = 45° :

	V	R.A.	D.	l.	b.	SGL	SGB
$V_{RF} - V_{MW}$	856	$12^{\text{h}} 48^{\text{m}}$	-35°	303°	$+28^{\circ}$	150°	-10°
$V_{VIR} - V_{RF}$	421	$02^{\text{h}} 20^{\text{m}}$	$+25^{\circ}$	148°	-33°	328°	-12°
$V_{VIR} - V_{LG}$	254	$11^{\text{h}} 52^{\text{m}}$	$+15^{\circ}$	253°	$+72^{\circ}$	096°	-10°

An infall velocity of about 400 km/sec in the direction of Virgo gives similar solutions. Note that there is no reason for the various vectors to be on the supergalactic plane. Schechter's solution for the Rubin-Ford effect shifts this vector, however, to about SGB = -45° .

The possibility exists that the velocity field is perturbed by not yet well studied, or more distant, density fluctuations (lack or excess of matter) so that an answer can be given only after we know more about the density distribution. Observationally, for instance, the effect of the large cloud at R.A. = $12^{\text{h}} 54^{\text{m}}$ and D. = $-15^{\circ} .2$, needs to be fully evaluated. The possibility also exists that the present difficulty is due to error or to large scale primordial vorticity of the Universe. It is therefore very important to have deep redshift surveys and understand the role played by the negative and positive perturbations. Theoretically

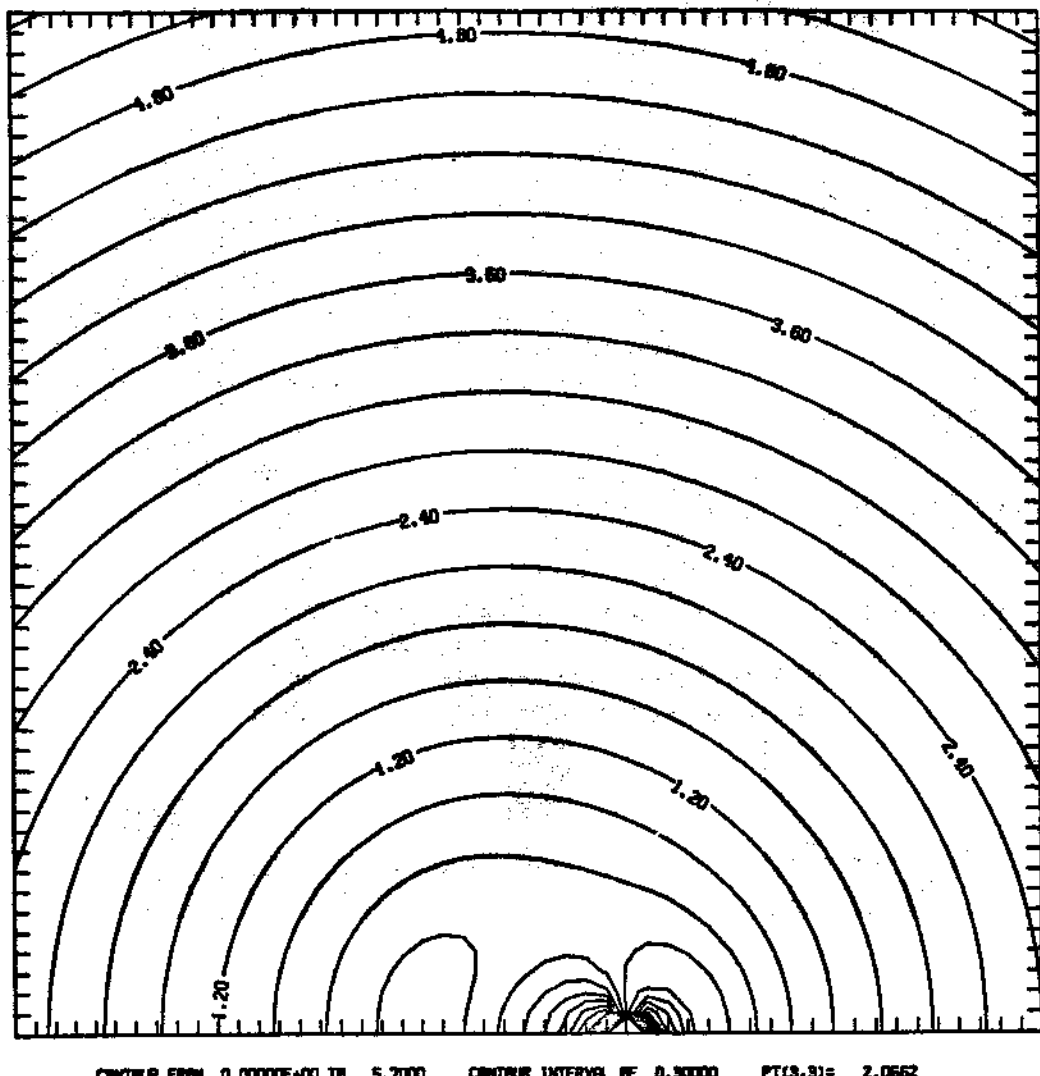
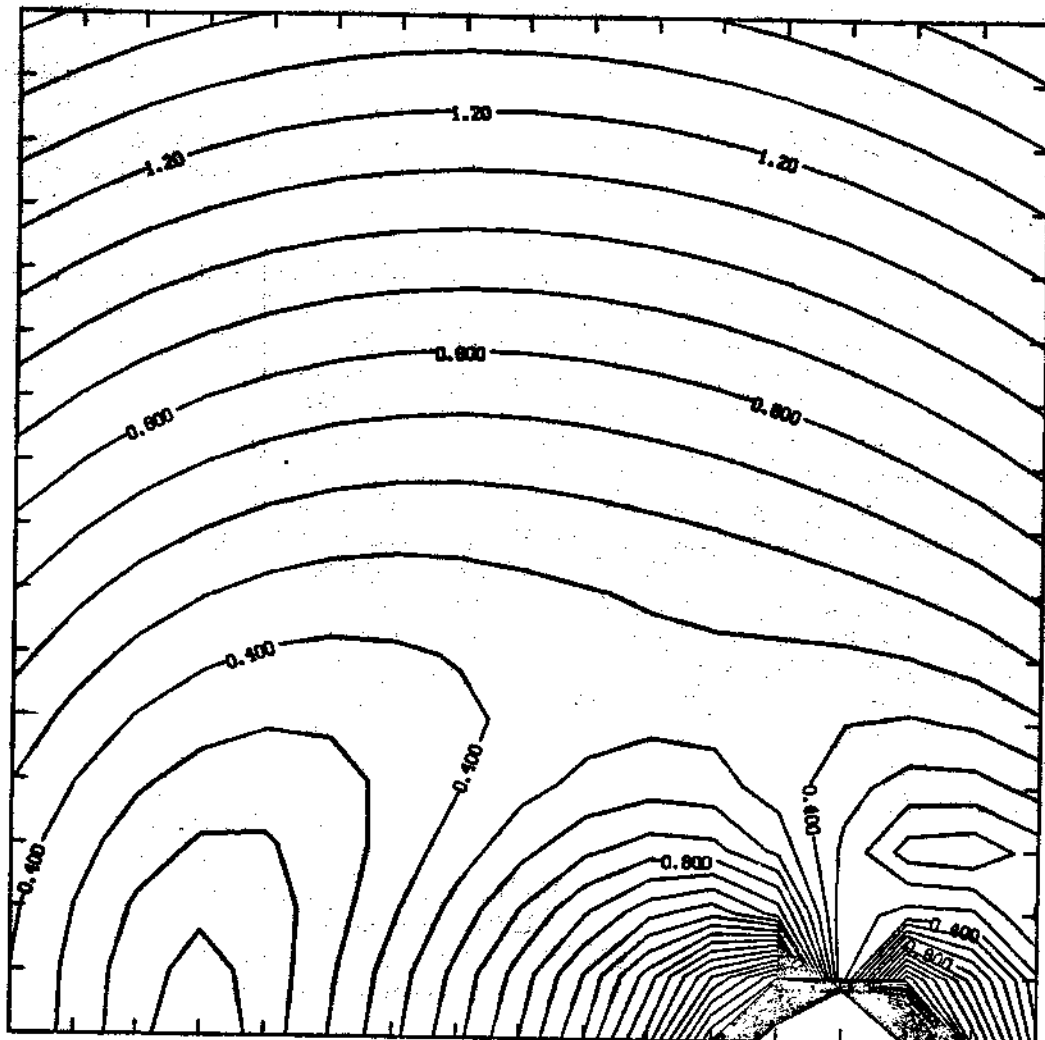


FIGURE 39 - The Hubble velocity field perturbed by a density excess $\delta\rho/\rho \propto R^{-2}$ centered in Virgo. The lines represent contours of equal velocities as seen from an observer at rest with the local group. The unit distance has been taken equal to the distance of Virgo. The infall velocity corresponds here to about 400 km/sec, $\delta\rho/\rho_0 = 0.4$. To convert to km/sec and Mpc, 10 thick marks correspond to the distance Virgo-Sun (about 20 Mpc) and the velocities to the Hubble flow at the distance of Virgo, $V_H = h \cdot d$ (multiply numbers on curve by about 20×50 km/sec).



CONTOUR FROM 0.0000E+00 TO 3.9000 CONTOUR INTERVAL OF 0.10000 PT(3,3)= 0.18763

FIGURE 40 - Same as figure 39. Here details are better visible. Note that the same redshift corresponds, in some directions, to various distances.

progress is being made in understanding the observed anisotropy in the microwave background.

VII - TOWARD MORE DETAILED PROPERTIES

From what I have said so far it is clear that a main emphasis is in the determination of peculiar velocities. To do this we need accurate redshifts and magnitudes. Using digitized spectroscopic data it is possible to achieve an accuracy of about 30 km/sec in good signal to noise low dispersion spectra (inverse dispersion of about 250 km/sec). Higher accuracy can be attained by radio 21 cm observations. Here we are, however, limited to the observations of spiral galaxies, morphological type later than S0. The redshift is generally determined to an accuracy of about 8 - 10 km/sec.

Using the Arecibo dish, 305 meter diameter with an HPBW of the antenna main lobe of about 3.3 arc min, the integration time is comparable to the exposure time needed for an optical spectrum and of about 10 - 20 minutes. Radio observations are a valid complement to optical observations not only because of the accuracy in redshift but because they give additional information which is important in understanding the formation and evolution of the large structure and the statistical characteristics of the member galaxies. From a 21 cm profile we can measure:

(1) redshift; (2) HI content and (3) total mass of the galaxy.

Projecting into the near future, knowledge of the galaxian mass will tell us about the mass distribution in these structures. A priori we would expect a random distribution because the same mechanism of galaxy formation should be at work in different parts of the supercluster and because the low density prevents the system from developing segregation through binary collision, for instance. On the other hand, as was also suggested in the work by Tarenghi et al. (1980) the formation of massive galaxies may be favored in regions where the density of the gas is higher.

Giovanelli, Haynes and myself are trying to answer this problem using the observations we are collecting in the region of the Perseus-Pisces supercluster. Our sample consists of about 1500 galaxies and we already have observations for about 1000 objects. The sample, which will be complemented by optical observations (E, SO galaxies) to allow a statistical analysis, has been carefully selected to gain detailed information on the supercluster structure and its kinematics. A preliminary indication or, at the present, a curiosity, is that the surface distribution of galaxies seems to be a function of the morphological type. In figure 41 we plot E/SO galaxies from the UGC catalogue. As can be seen they define a rather narrow structure, a filament in space. Such narrow structure, the supercluster spine, is gradually lost if we go to later morphological types. The extreme is shown in figure 42 where we plot the surface distribution of dwarf galaxies. The sample used here is spurious, that is galaxies have not been selected by redshift so that the supercluster is contaminated by foreground and background objects. The contamination could be particularly strong for dwarf galaxies since, due to their fainter absolute magnitude, they could be part of the foreground.

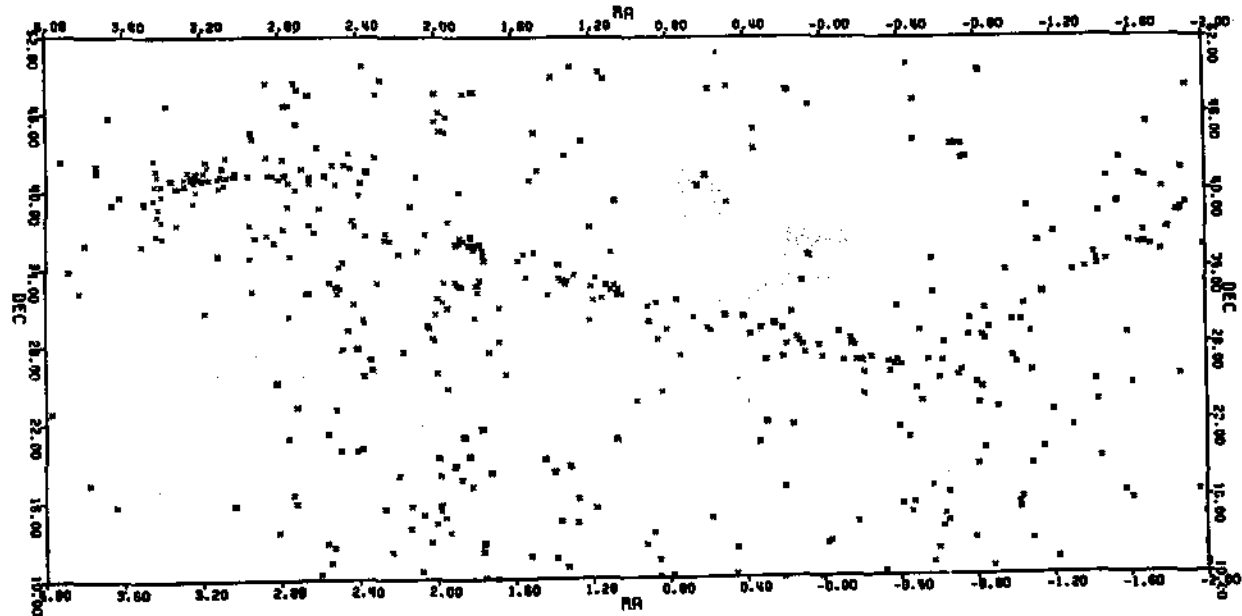


FIGURE 41 - E/SO galaxies in the Perseus-Pisces supercluster. These galaxies define a rather sharp spine which extends over about 90° of the sky.

The preliminary results of our survey, however, show that most of the galaxies, including the dwarfs and irregulars, are indeed at a distance of about 5000 km/sec, the distance of the Perseus-Pisces supercluster. This structure extends over about 90 degrees of the sky and for a length of about 100 Mpc.

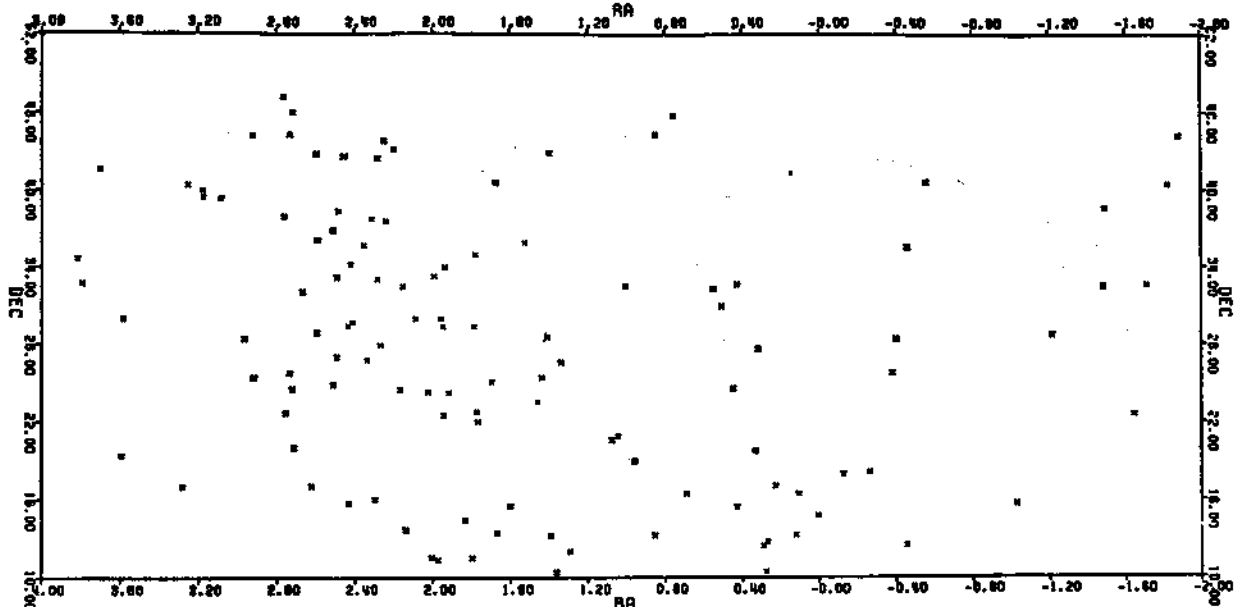


FIGURE 42 - The structure as seen in Figure 41 goes practically undetected at later morphological types. Here we show the distribution of dwarf galaxies. The present sample is however spurious since I have plotted UGC galaxies so that the plots are somewhat affected by foreground/background contaminations.

Following the understanding of the distribution of matter the interaction between its forms becomes of basic importance during the process of formation and evolution. Progress is being rapidly made in this unlimited field. I open here a parenthesis to describe the interaction between the intergalaxian gas and the galaxies since such information may have bearing on the understanding of the evolution of the superclusters and their content.

Statistically the HI content or better the distance independent radio MHI/L is a function of the morphological type. The correlation MHI/L - Galaxian type has been discussed by Roberts (1975) and Balkowski (1973). More recently Giovanelli and Haynes observed a selected sample of isolated galaxies with the Arecibo telescope (Haynes et al., 1981), this is the sample I will refer to as standard sample (*). The HI content of a galaxy is a function not only of its formation and evolution, but also the result of the interaction with its environment. A galaxy may in fact interact tidally with another galaxy or with the intergalactic medium. In the latter case only the gas component of the galaxy, interstellar medium, is affected. The main mechanisms at work are:

- (1) tidal interaction;
- (2) sweeping: a galaxy in relative motion with respect to a gaseous medium will be subjected to a pressure $P = \delta V^2$ where δ is the density of the medium in which the galaxy is moving and V its relative velocity;
- (3) Evaporation: the interstellar gas of a galaxy embedded in a hot gas is heated by conduction. The gas changes state and evaporates, Spitzer , Cowie et al. (1977).

It is clear a priori that such depletion mechanisms are particularly effective in clusters of galaxies since:

(*) Note that standard means the same content of neutral hydrogen per unit luminosity as galaxies in the standard sample. The sample of isolated galaxies is probably composed of galaxies which belong to low density supercluster regions. The value of the deficiency, therefore, detects fluctuations over a mean value. In noncluster regions the relative differences (gradient) is a more sensitive parameter.

- (a) the number density of galaxies is high;
 - (b) the velocity dispersion (virial velocity) of the galaxies relative to the medium is of the order of 1000 km/sec;
 - (c) the temperature of the gas, as determined by x-ray observations, is of the order of magnitude needed for conduction to be efficient, $T = 10^7$ °K.
- Tidal interaction, however, may not be an efficient mechanism in this context since:
- (1) the number of collisions a galaxy suffers is rather small;
 - (2) quite often the measured HI deficiency is larger than we would expect from a tidal effect;
 - (3) deficient galaxies are not restricted so much to the core region as seems to occur for galaxies which have been affected by tidal phenomena (Strom et al., 1978).

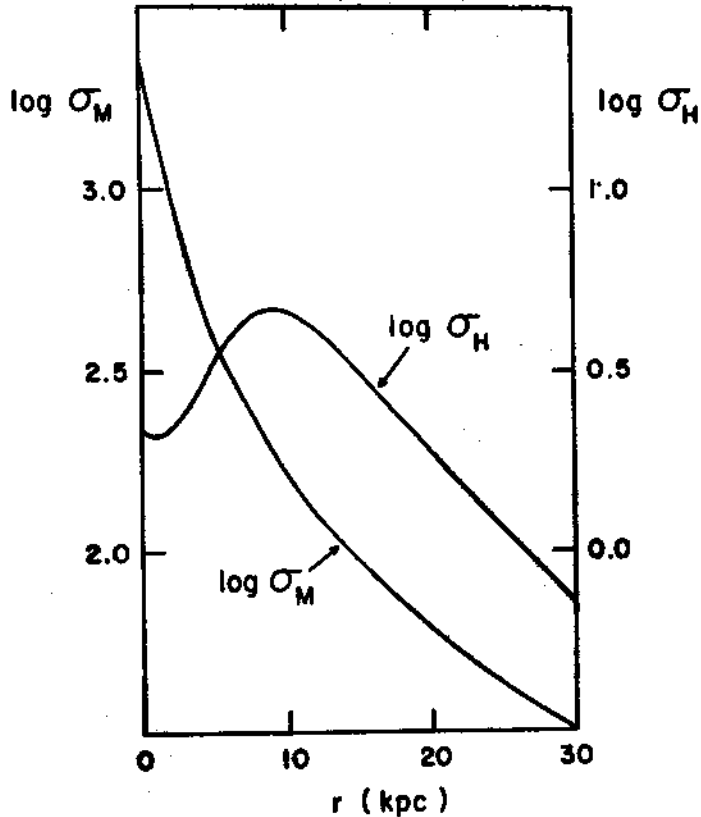


FIGURE 43 - Synthetic curves for the total mass surface density (σ_M) and the HI surface density (σ_H), in $M_0 \text{ kpc}^{-2}$, obtained by averaging the observationally determined curves of the galaxies NGC 2841, M31, NGC 5033, NGC 7331, NGC 5055, and IC 342, after Bosma (1978).

ficiency which is related to cluster phenomena while supercluster galaxies, dispersed component, have, within the errors of the observations and in a statistical sense, a standard hydrogen content.

(*) In some cases the HI is not detected in the galaxy. In these cases we measure the RMS of the radio noise and determine an upper limit for the hydrogen mass. The value of the upper limit is treated in the analysis as a detected value, longer integration would enhance the effect discussed.

All of these effects are small in the low density regions of a supercluster where the motion of a galaxy relative to other galaxies or to the cold gas is small. In these regions galaxies may be accreting material, an effect, however, difficult to evidence observationally. Neutral hydrogen is a good probe because, due to its extended distribution, Fig. 43 it is particularly sensitive to all of these interactions and its galaxian content is a measurable quantity. The parameter used for the analysis is the hydrogen deficiency (*) is defined as:

$$\text{DEF} = \log \langle M_H/L \rangle_{\text{ST}} - \log (M_H/L) \quad (39)$$

for each galaxy type.

Figure 44, 45 show that a deficiency is observed in clusters which are members of the Hercules Supercluster. No deficiency is observed in supercluster galaxies which are believed to be members of the noncluster component (Giovanelli et al., 1981). The same effect is illustrated in Figure 46 for the Coma A1367, figure 47, supercluster (Chincarini et al., 1982; Sullivan, et al., 1981). The deficiency parameter peaks in the cluster region. The observations, however, are not sensitive to small gradients which may be present in the dispersed component. The observations show, therefore, that cluster galaxies have a detectable de-

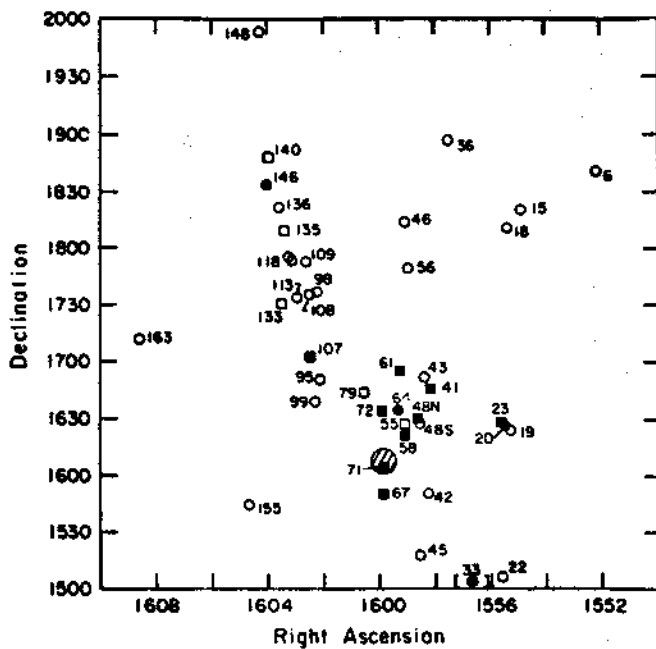


FIGURE 44 - The Hercules supercluster region in the CGCG field 108. Unfilled circles, detected galaxies with $\text{Def} > 0.48$; unfilled squares, undetected galaxies with lower limit of $\text{Def} < 0.48$ (galaxies observed for relatively insufficient integration times are in this group); filled squares, undetected galaxies with lower limits of $\text{Def} > 0.48$. The X-ray source in A2147 is represented by a circle with radius roughly representative of the isothermal core radius as reported by Jones et al. (1979). The numbers by each symbol identify the galaxies by their CGCG order in the field 108.

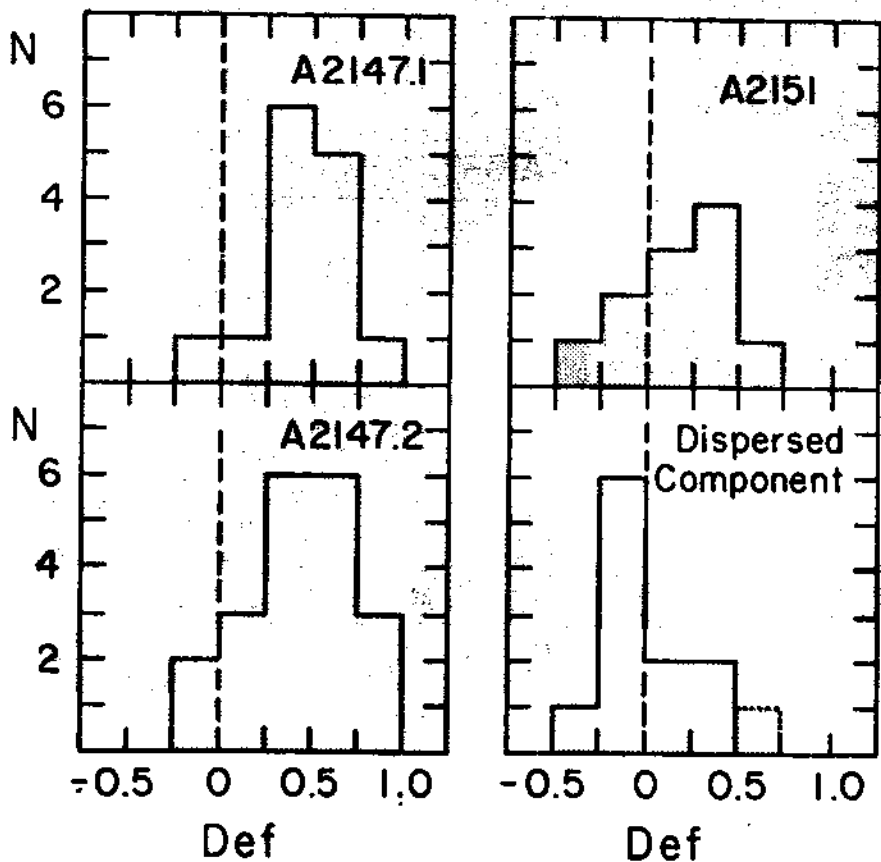


FIGURE 45 - Distribution of the deficiency parameter Def in four different groups of the Hercules supercluster, as defined in the text. The galaxy entered within dashed contours is Zw 108 - 033, for which the morphology is uncertain.

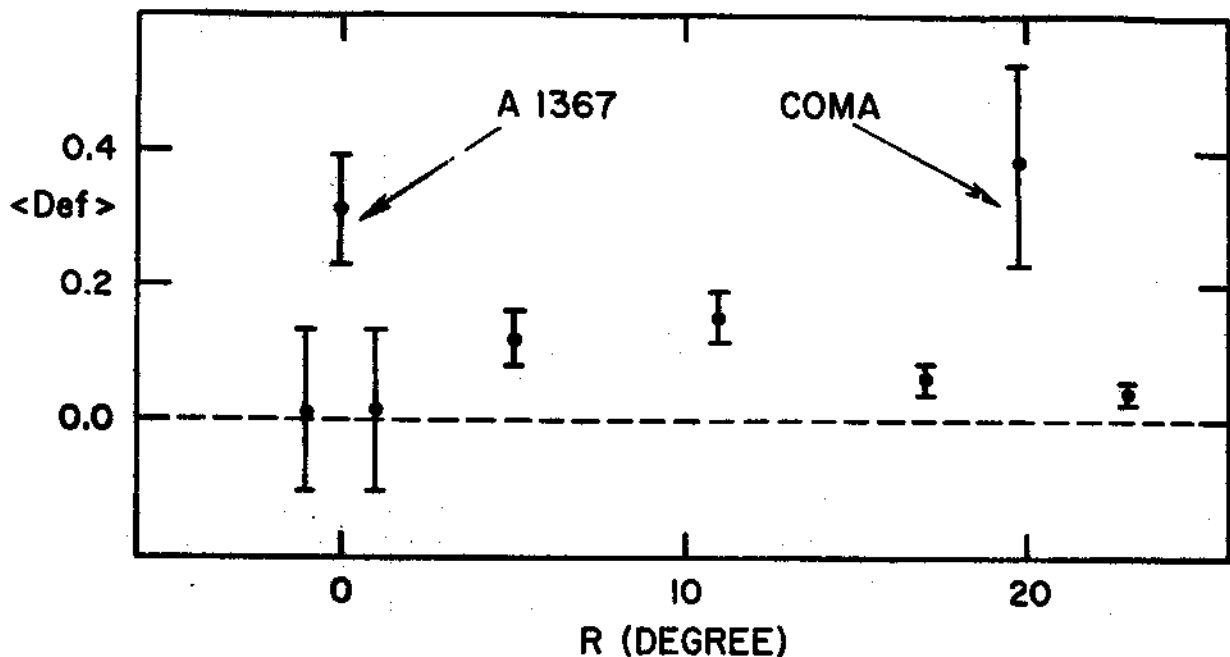


FIGURE 46 - Deficiency parameter in the region between A1367 and Coma as a function of the distance from the A1367 cluster.

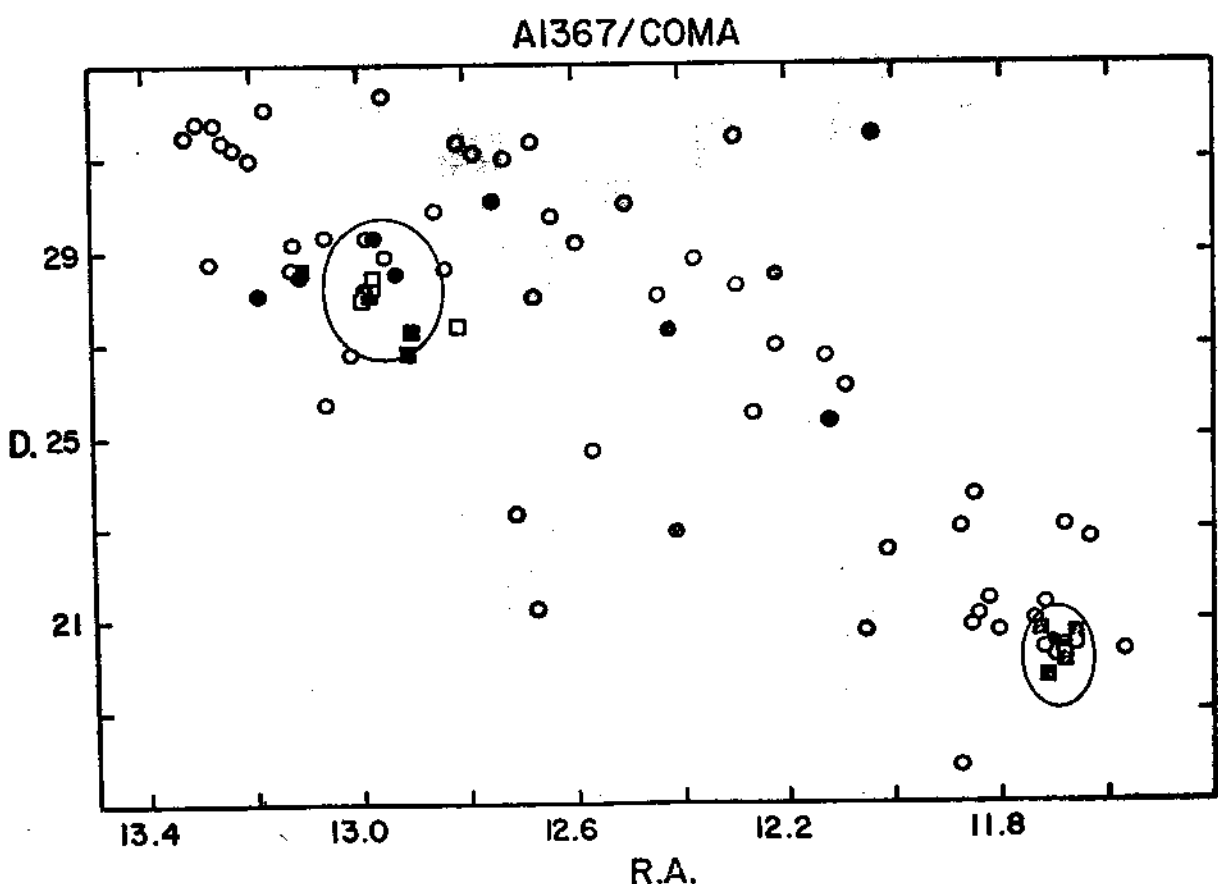


FIGURE 47 - Distribution of the galaxies observed in 21 cm between Coma and A1367.

The hydrogen deficiency affects the stellar evolution and the morphology of galaxies. There may be also some indication (Chincarini et al., 1982) that the interaction with the intracluster medium started when galaxies were still rather young. This would imply that the intracluster gas is, at least in part, primordial (the presence of lines due to heavy elements in the X-ray spectrum assures us that a large part of it is due to mass loss from the galaxies). Such possibility is reasonable, since we hardly expect mechanism of galaxy formation which is 100% efficient, and in agreement with the fact we may have gas along the supercluster structure.

VIII - CONCLUSION

In these lectures I tried to illustrate the distribution of visible matter in the universe. The evidence is growing that all galaxies are part of large structures of superclusters. The superclusters are not bound or dynamically rotating units but are rather massive agglomerates which expand with the expansion due to the Hubble flow and the breaking action exerted by their mass. In between superclusters we observe large voids or regions where the density of galaxies is very small. Such voids should act as negative fluctuations on the surrounding regions. The geometry of the structures and of the voids is not well defined. The superclusters as defined above, seem to be the largest structures, of the order of 50 - 100 Mpc, we observe in the universe. Voids seem to be of comparable sizes. Clusters and groups of galaxies form substructures which are embedded in the superclusters. Galaxies prefer the company of other galaxies.

The relevance of these large scale structures to cosmology open the theoretical chapter of their formation and evolution and the related investigations of the distribution of matter at large redshifts and as evidenced from surveys in other frequencies. The theory may have difficulties in explaining structures which are much larger than 50 Mpc, on the other hand the fast development in this field and a better understanding of the observational data may give us enlightened understanding, and additional problems, in the near future. It is clear, in fact, that assuming the distribution given by the autocorrelation function a 50 Mpc structure implies a fluctuation. The fluctuation is fading in the backgrounds. To reconcile this with the 100 Mpc size structures we note that:

- (a) A redshift survey is able to discern structures at a very low density level since such structures are separated by regions which are void of galaxies to the limiting magnitude of the samples so far available.
- b - Such structures may be rather rare. It is however a fact we are detecting them in all the regions of the sky so far observed (selection effect?).
- c - At large scale sizes we are not necessarily measuring the same thing. The autocorrelation scale length may characterize substructures in the three dimension supercluster.

In other words it may be simply a matter of nomenclature of definition of the redshift detected large structures. Whether superclusters are detectable at very large distances is uncertain. Oort et al. suggest superclustering of quasars while Osmer (1981) finds that there is no evidence of clustering. The most recent work by Sargent et al. (1982) invalidates the interpretation of Oort et al..

APPENDIX 1

Assume that all galaxies are in clusters with a density distribution of the type $R^{-\epsilon}$ (this is valid at large distances from the cluster center where an isothermal distribution can be approximated by the law $\rho(R) \propto R^{-2}$). In this case we can write using the approximation for a continuous fluid:

$$\langle n \rangle^2 [1 + \xi(\tau)] = \langle \rho(R)\rho(R + \tau) \rangle = \int d^3R \rho(R)\rho(R + \tau)$$

with: $d^3R \approx dR^2 d\Omega$; $d\Omega$ is the solid angle

$$(R + \tau)^2 = R^2 + \tau^2 - 2R\tau \cos \theta$$

$$\langle n^2 \rangle \left| 1 + \xi(\tau) \right| \approx \int_{-1}^{+1} d\cos \theta \int_0^\infty dR R^{2-\epsilon} (R^2 + \tau^2 - 2R\tau \cos \theta)^{-\epsilon/2}$$

using $y = R/\tau$

$$\approx \tau^{3-2\epsilon} \int_{-1}^{+1} d\cos \theta \int_0^\infty dy y^{2-\epsilon} (y^2 + 1 - 2y \cos \theta)^{-\epsilon/2} = \tau^{3-2\epsilon} I(\epsilon)$$

so that for $\xi(\tau) \gg 1$

$$\rho(R) \approx R^{-\epsilon} \text{ and } \xi(R) \approx R^{3-2\epsilon}$$

for $\epsilon = 2$

$$\rho(R) \approx R^{-2} \text{ and } \xi(R) \approx R^{-1}$$

(The example is due to Marc Davis).

APPENDIX 2

The complete Gamma function is defined as:

$$\Gamma(a) = \int_0^\infty e^{-t} t^{a-1} dt, \quad a > 0$$

and the incomplete Gamma function as:

$$\Gamma(a, x) = \int_0^x e^{-t} t^{a-1} dt$$

The number of objects in an ensemble of galaxies is given by (*):

$$N = \int_0^\infty \Phi(L) dL = \Phi' \Gamma(a + 1)$$

The total luminosity

$$L_{TOT} = \int_0^\infty L \Phi(L) dL = \Phi' L' \Gamma(a + 2)$$

The number of objects brighter than L

$$\int_L^\infty \Phi(L) dL = \Phi' \Gamma(a + 1, L/L')$$

and the luminosity due to objects brighter than L

$$\int_L^\infty L \Phi(L) dL = \Phi' L' \Gamma(a + 2, L/L')$$

At faint luminosities the function is however poorly known. There are no data for cluster galaxies fainter than $M = -16.0$. Tammann and Kran using a sample of galaxies within 9.1 Mpc ($V_0 < 500 \text{ km sec}^{-1}$) state that the luminosity function may peak at about $M = -15.7$ and simulate a Gaussian distribution with $\sigma(M) = 3.3$. At this magnitude the sample is dominated by S/Irr galaxies (E/SO have a rather flat distribution). Different luminosity functions have been found for the various morphological types, Holmberg (1975) and Yahil et al. (1980) and yet the composite luminosity function seems to be a cosmic constant in spite of the variations in the content of galaxies (morphological types) from cluster to cluster and between cluster and non-cluster regions. Such constancy, when no distinction is made for morphological type, must reflect the constancy in the mass (luminosity) distribution during the process of formation. Morphology may be a feature (not so essential) added during the process of formation and evolution and dependent on the galaxian environment.

(*) Since $(a+1)$ is negative one can use $\Gamma(a+1) = \Gamma(a+1, L_{MIN}/L')$, where L_{MIN} can be, for instance $L_{MIN} = 10^{-04}(-10-M_0)$ or use Abell's luminosity function.

For some practical purposes the great cluster function is extrapolated to infinity or to $M \leq -10$, about the luminosity of one of brightest globular clusters.

APPENDIX 3

The number of galaxies brighter than the apparent magnitude m is given by:

$$N(< m) = C 10^{-0.6m}$$

If we assume to represent the uniform background by this equation, an upper limit for C can be derived from observations of a noncluster sample of redshifts. In this case if we observe N galaxies in the redshift range V_i, V_j

$$N(0, \infty) = N(\leq m) = C 10^{-0.6m_1} = N_{\text{sample}}$$

and if we have

$$N(V_i, V_j)_{\text{GAP}} / N(0, \infty)_{\text{OBS}} \ll N(V_i, V_j)_{\text{expected}} / N(0, \infty)_{\text{THEO}}$$

we can write

$$N(V_i, V_j)_{\text{GAP}} / N(0, \infty)_{\text{BGD}} \geq A = N(V_i, V_j)_{\text{THEO}} / N(0, \infty)_{\text{THEO}}$$

from which we have

$$N(0, \infty)_{\text{BGD}} \leq N(V_i, V_j)_{\text{GAP}} / A$$

(\leq ; if there is no object in the GAP we can use $N(V_i, V_j)_{\text{GAP}} = 1$) and

$$C \leq N(0, \infty)_{\text{BGD}} / 10^{-0.6m_1} = N(V_i, V_j)_{\text{GAP}} / (A 10^{-0.6m_1})$$

APPENDIX 4

The luminosity of the region of the structure observed can be determined using the Model described after the free parameters have been derived from the best fitting with the observations. We can, in fact, estimate:

$$\Omega D_0 / \sqrt{2\pi} = N_{\text{TOT}} / \int_0^{\infty} x^2 \sqrt{2\pi} D(x) \Gamma(a + 1, L/L') / D_0 dx$$

and

$$L_{\text{tot}}^{(\text{tot})} = \Omega D_0 / \sqrt{2\pi} \int_0^{\infty} x^2 / D_0 \sqrt{2\pi} D(x) \Gamma(a + 2) L' dx$$

where Ω = solid angle of the observed region N_{tot} = total number of observed objects.

In a more direct way and model independent: consider galaxies which are in a shell at a distance L , the luminosity of the shell is: $L_{\text{OBS}} = \sum_i L_i$, where L_i is the luminosity of the galaxy and since the sample is magnitude limited, we have

$$L_{\text{tot}}^{(\text{shell})} = L_{\text{OBS}} \int_0^{\infty} L \phi(L) dL / \int_L^{\infty} L \phi(L) dL = \Gamma(a + 2) / \Gamma(a + 2, L/L')$$

Since each sample galaxy (m_i, z_i) defines its own shell we can write:

$$L_{\text{tot}} = \sum_i L_i \Gamma(a + 2) / \Gamma(a + 2, L_i / L')$$

where L_i / L' is determined once m_i and z_i are known.

APPENDIX 5

Assigning membership to the cluster dispersed component is analogous to assigning membership. The dispersed component has been defined, in fact, as the ensemble of galaxies which are non-cluster members.

A useful approach is the one used by Materne et al. (1980) where a membership probability has been assigned to each galaxy as a function of its redshift and space distribution. Another convenient approach, since in a supercluster we are working with a sample of galaxies which are within a rather limited range of redshifts, is the one devised by Gott and Turner (1976). The density enhancement is detected as that are where the number density of objects is larger than a chosen value, Fig. A4.1. The region I have chosen as an example refers to the area of the cluster A262. The velocity dispersion for the component along the line of sight is $\sigma = 615$ km/sec (a much smaller dispersion is determined from the E, SO galaxies which are concentrated toward the cluster center, $V = 262$). The velocity dispersion along the line of sight for galaxies which are outside the cluster are ($1^{\text{h}}40^{\text{m}} < \text{RA} < 2^{\text{h}}0^{\text{m}}$ and $34^{\circ} < \text{D} < 38^{\circ}$) is in the range of 400 to 500 km/sec for various regions of the sky. The latter dispersion is interpreted as due to the supercluster depth. Clearly in this and similar cases contamination by non members is unavoidable. We also face a serious difficulty in deciding whether or not a density enhancement is unbound and expanding. A problem which is of very great cosmological interest.

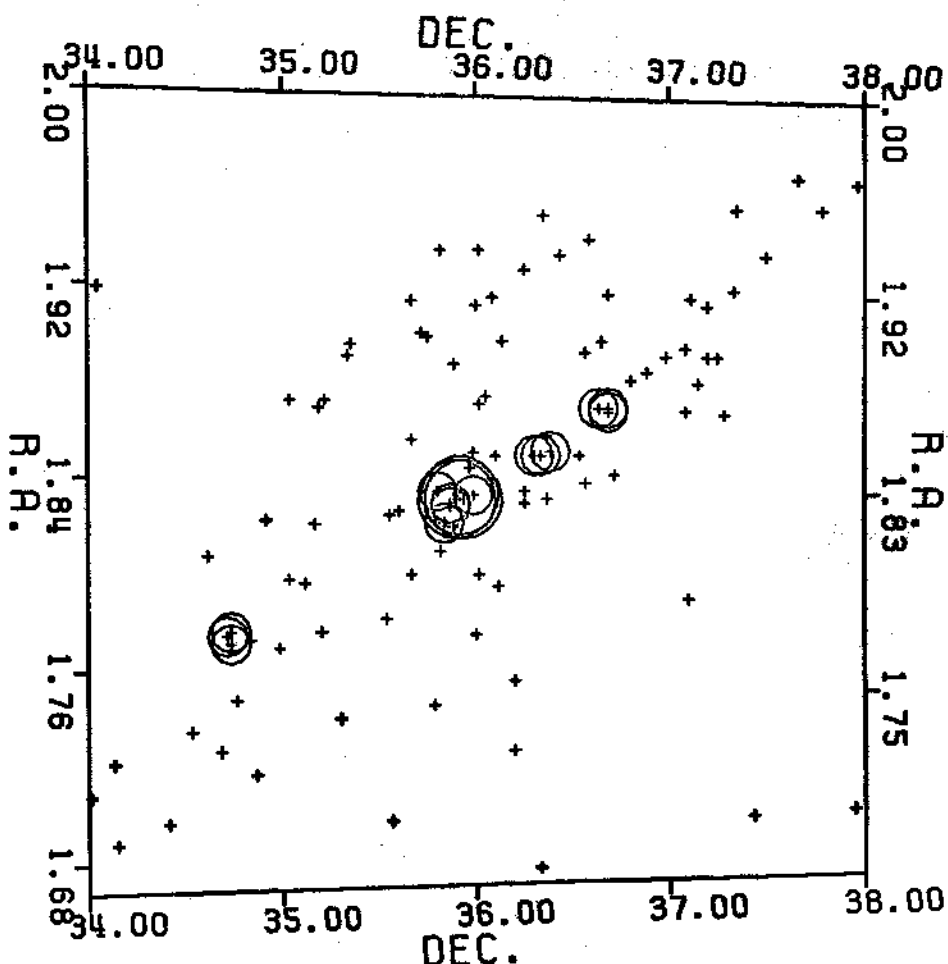


FIGURE A4.1 - Density enhancement in the region of the cluster A262. Centering on each object and varying the radius of the circle we can select regions which are above a selected threshold density.

ACKNOWLEDGEMENTS

I give my thanks to my colleague David Branch for reading the manuscript and for his discussions; and Linda Fannin for the patient and dedicated work in typing the manuscript. Thanks to Linda Barker for great help with parts of the figures made by computer.

REFERENCES

- 1 - Hubble, E.P., 1934, Ap. J., 79, 8.
- 2 - Shapley, H. and Ames, A., 1932, Harvard Obs. Ann. 88, n° 2.
- 3 - Vaucouleurs, G.H.de, 1956, Vistas Astron., 2, 1584.
- 4 - Zwicky, F., 1970, Private Communication.
- 5 - Zwicky, F., Wild, P., Herzog, E., Karpowicz, M., Koval, C., 1961-1968, Catalogue of Galaxies and Clusters of Galaxies, vol. 1-6, California Institute of Technology, Pasadena.
- 6 - Abell, G., 1958, Ap.J.SuppL., 3, 211.
- 7 - Shane, C.D. and Wirtanen, C.A., 1967, Publ.Lick Obs., 22, Pt. I.
- 8 - Shane, C.D. and Wirtanen, C.A., 1954, A.J., 59, 285.
- 9 - Haynes, M.P. and Giovanelli, R., Meeting of the A.A.S. in Boulder, Colorado, Jan., 1982.
- 10- Rudnicki, K., Dworak, T.Z., Flin, P., Baranowski, B. and Sendrakowski, A., 1973, Acta Cosmologica, 1, 7.
- 11- Geyer, E.H., Joffman, M. and Nelles, B., 1979, A.A., 80, 248.
- 12- Angel, R., 1980, Private Communication.
- 13- Neymann, Scott, and Shane, 1953, Ap.J., 117, 92.
- 14- Peebles, P.J.E., 1980, The Large-Scale Structure of the Universe. Princeton Series in Physics and references therein.
- 15- Totsuji, H., and Kiara, T., 1969, Publ.Astron.Soc.Japan, 21, 221.
- 16- Abell, G., 1962, Problems of Extragalactic Research, ed.G.C.McVitlie.
- 17- Schechter, P., 1976, Ap.J., 203, 297.
- 18- Felten, J.E., 1977, Goddard Space Flight Center, preprint x-602-77-162 A.J.82,861.
- 19- Zwicky, F., 1957, Morphological Astronomy (Berlin: Springer-Verlag).
- 20- Mayall, N.U., 1960, Annales d'Astrophysique, 23, 344.
- 21- Chincarini, G., 1978, Nature, 272, 515.
- 22- Chincarini, G. and Martin, D.H., 1975, Ap.J., 196, 335.
- 23- Gregory, S.A. and Thompson, L.A., 1978, Ap.J., 222, 784.
- 24- Einasto, J., Joeveer, Mn. Saar, E., 1980, M.N.R.A.S., 193, 353.
- 25- Zeldovich, Ya. B., 1970, A.A., 5, 84.
- 26- Chincarini, G., Giovanelli, R. and Haunes, M., 1981, preprint.
- 27- Oort, J.H., Arp, H.C., DeRuiter, H., 1981, A.A., 95, 7.
- 28- Sargent, W.L.W., Young, P.J. and Schneider, D.P., 1982, preprint.
- 29- Kirshner, R.P., Oemler, A.Jr., and Schechter, P.L., 1979, A.J., 84, 951.
- 30- Kirshner, R.P., Oemler, A.Jr., Schechter, P.L. and Schectman, S.A., 1981, Ap.J., 248-L57.
- 31- Corwin, H., 1980, Private Communication, Dissertation.
- 32- Schuch, N.J., 1981, M.N.R.A.S., 196, 695.
- 33- Geller, M.J. and Peebles, P.J.E., 1973, Ap.J., 194, 329.
- 34- Tammann, G.A., Sandage, A. and Yahil, A., 1980, Les Houches, Physical Cosmology, North-Holland Publishing Company.
- 35- Rubin, V.C., Thonnard, N., Ford, W.K. and Roberts, M.S., 1976, A.J., 81, 719.
- 36- Braduardi, Raymont, G., Fabricant, D., Feigelson, E., Gorenstein, P., Grindlay, J., Soltan, A. and Zamorani, G., 1981, Ap.J., 248-55.
- 37- MacGillivray, H.T., Martin, R., Pratt, N.M., Reddish, V.C., Seddon, H., Alexander, L.W.G., Waller, G.S. and Williams, P.R., 1976, M.N.R.A.S., 176, 649.
- 38- Schipper, L., King, I.R., 1978, Ap.J., 220, 798.
- 39- Carter, D., Metcalfe, N., 1980, M.N.R.A.S., 191, 325.
- 40- Binggeli, G., 1981, preprint.
- 41- deVaucouleurs, G., 1953, A.J., 58, 30.
- 42- Tully, B.R., 1981, preprint.
- 43- Binney, J. and Silk, J., 1979, M.N.R.A.S., 188, 273.
- 44- Yahil, A., Sandage, A., and Tammann, G.A., 1980, Les Houches, Physical Cosmology, North-Holland Publishing Company.
- 45- Davis, M. and Huchra, J., 1981, preprint N.1510 (Center for Astrophysics)

- 46- Aaranson, M., Mould, J., Huchra, J., Sullivan, W.T., Schommer, P.H. and Bothum, G.C., 1980, Ap.J., 239, 12.
- 47- Schechter, P.L., 1980, A.J., 85, 801.
- 48- Sandage and Tamman, Preprint ESO, N.174.
- 49- Clutton-Brock, M. and Peebles, P.J.E., 1981, A.J., 86, 1115.
- 50- Visvanathan, N., 1979, Ap. J., 228, 81.
- 51- Schechter, P.L., 1977, A.J., 82, 569.
- 52- Tarenghi, M., Chincarini, G., Rood, H.J. and Thompson, L.A., 1980, Ap.J., 235, 724; Appendix, Maternet et al.
- 53- Roberts, M.S., 1975, in Galaxies and the Universe, ed. A.Sandage, M.Sandage and J. Kristian (Chicago: University of Chicago Press).
- 54- Balkowski, C., 1973, A.A., 29, 43.
- 55- Haynes, M. and Giovanelli, R., 1981, to be published.
- 56- Spitzer, Lr.Jr., Ap.J., 124, 20.
- 57- Cowie, L.L. and McKee, C.F., 1977, Ap.J., 211, 135.
- 58- Strom, K.M. and Strom, S.E., 1978, Ap.J., 225, L93.
- 59- Giovanelli, R., Chincarini, G., Haunes, M.P., 1981, Ap.J., 247, 383.
- 60- Chincarini, G., Giovanelli, R. and Haynes, M., 1982, to be published.
- 61- Sullivan, W.T. III, Bothum, G.D., Bates, B. and Schommer, R.A., 1981, A.J., 86, 919.
- 62- Osmer, P.S., 1981, Ap.J., 247, 762.
- 63- Holmberg, E., 1975, Galaxies and the Universe, edited by Sandage, Sandage and Kristian. University of Chicago Press.
- 64- Turner, E.L. and Gott, J.R., 1976, Ap.J. Suppl. Series, 32, 409.